Earth-Science Reviews 211 (2020) 103433

Contents lists available at ScienceDirect

Earth-Science Reviews

journal homepage: www.elsevier.com/locate/earscirev

The status and stability of permafrost carbon on the Tibetan Plateau

Cuicui Mu [a,b,c,e,g], Benjamin W. Abbott [d], Adam J. Norris [d], Mei Mu [a], Chenyan Fan [a], Xu Chen [a], Lin Jia [a], Ruimin Yang [a], Tingjun Zhang [a], Kang Wang [f], Xiaoqing Peng [a,g], Qingbai Wu [c], Georg Guggenberger [h], Xiaodong Wu [b,i,*]

[a] *Key Laboratory of Western China's Environmental Systems (Ministry of Education), College of Earth and Environmental Sciences, Lanzhou University, Lanzhou 730000, China*

[b] *Cryosphere Research Station on Qinghai-Tibetan Plateau, State Key Laboratory of Cryospheric Science, Northwest Institute of Eco-Environment and Resource, Chinese Academy of Sciences, Lanzhou 730000, China*

[c] *State Key Laboratory of frozen soil engineering, Northwest Institute of Eco-Environment and Resource, Chinese Academy of Sciences, Lanzhou 730000, China*

[d] *Department of Plant and Wildlife Sciences, Brigham Young University, Provo, UT 84602, USA*

[e] *Southern Marine Science and Engineering Guangdong Laboratory, Zhuhai 519000, China*

[f] *School of Geographic Sciences, East China Normal University, Shanghai 200241, China*

[g] *University Cooperation of Polar Research, Beijing 100875, China*

[h] *Institute of Soil Science, Leibniz Universität Hannover, Herrenhäuser Straße 2, 30419 Hannover, Germany*

[i] *University of Chinese Academy of Sciences, Beijing 100049, China*

A R T I C L E I N F O

Keywords:
Soil organic carbon
greenhouse gas
temperature sensitivity
thaw slumps, thermokarst lakes
permafrost
Tibetan Plateau

A B S T R A C T

Permafrost regions at high latitudes and altitudes store about half of the Earth's soil organic carbon (SOC). These areas are also some of the most intensely affected by anthropogenic climate change. The Tibetan Plateau or Third Pole (TP) contains most of the world's alpine permafrost, yet there remains substantial uncertainty about the role of this region in regulating the overall permafrost climate feedback. Here, we review the thermal and biogeochemical status of permafrost on the TP, with a particular focus on SOC stocks and vulnerability in the face of climate warming. SOC storage in permafrost-affected regions of the TP is estimated to be 19.0±6.6 Pg to a depth of 2 m. The distribution of this SOC on the TP is strongly associated with active layer thickness, soil moisture, soil texture, topographic position, and thickness of weathered parent material. The mean temperature sensitivity coefficient (Q_{10}) of SOC decomposition is 9.2±7.1 across different soil depths and under different land-cover types, suggesting that carbon on the TP is very vulnerable to climate change. While the TP ecosystem currently is a net carbon sink, climate change will likely increase ecosystem respiration and may weaken or reverse the sink function of this region in the future. Although the TP has less ground ice than high latitude permafrost regions, the rugged topography makes it vulnerable to widespread permafrost collapse and thermo-erosion (thermokarst), which accelerates carbon losses. To reduce uncertainty about SOC quantities and sensitivity to warming, future studies are needed that explain variation in Q_{10} (e.g. based on SOC source or depositional position) and quantify the role of nutrient availability in regulating SOC dynamics and ecosystem recovery following disturbance. Additionally, as for the high latitude permafrost region, soil moisture and thermokarst formation remain major challenges to predicting the permafrost climate feedback on the TP. We present a conceptual model for of greenhouse gas release from the TP and outline the empirical observations and modeling approaches needed to test it.

1. Introduction

Permafrost is one of the major components of the Earth system, underlying approximately 21% of the exposed land area in the Northern Hemisphere (Obu et al., 2019). Permafrost regions have accumulated globally relevant amounts of organic matter, with permafrost-affected soils in the Northern Hemisphere estimated to hold approximately 50% of the global soil organic carbon (SOC) (Hugelius et al., 2014; Tarnocai et al., 2009). Current estimates of permafrost-region SOC pools are 1307 ± 170 Pg, of which 472 ± 27 Pg C is distributed in the upper 1

* Corresponding author.
E-mail address: wuxd@lzb.ac.cn (X. Wu).

https://doi.org/10.1016/j.earscirev.2020.103433
Received 20 August 2020; Received in revised form 25 October 2020; Accepted 1 November 2020
Available online 4 November 2020
0012-8252/© 2020 Elsevier B.V. All rights reserved.

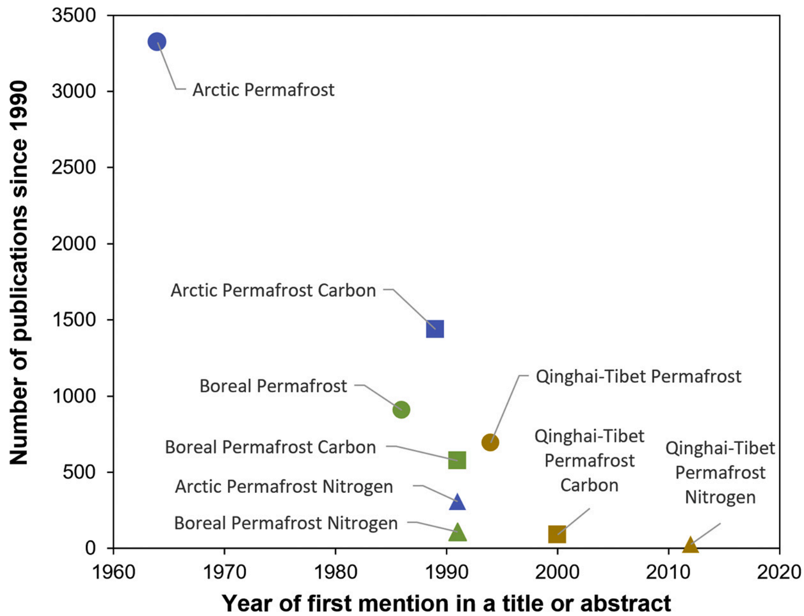

Fig. 1. Results from a meta-analysis of the number of publications mentioning Arctic, Boreal, and Tibetan Plateau permafrost and other terms. We used the Web of Science database to perform the search.

m of soils, and 1035 ± 150 Pg C is in the upper 3 m (Hugelius et al., 2014). The decomposition of permafrost organic matter produces CO_2, CH_4, and N_2O (Treat et al., 2014), depending on the redox conditions and type of microbial metabolism. Consequently, it is crucial to better quantify the amount of organic matter in permafrost, its degree of exposure to microbial activity, and its sensitivity to warming to accurately project future greenhouse gas trajectories and achieve global climate targets (McGuire et al., 2018; Abbott et al., 2016).

Besides containing much of the Earth's organic matter, permafrost regions are also experiencing some of the fastest climate change. The surface air temperature in the Alaskan Arctic warmed at 0.71°C per decade over 1998–2015 (Wang et al., 2017), and on the Tibetan Plateau or "Third Pole" (TP), air temperature has increased by 0.40–0.52°C per decade since the 1980s (Cheng et al., 2019). The enhanced warming of the permafrost zone is attributable to factors that preferentially increase the net flux of energy to the surface along elevation and latitudinal gradients, such as snow-albedo feedbacks, cloud-radiation effects, aerosols, and ozone-depleting gases (Pepin et al., 2015; Polvani et al., 2020). This rapid climate change has triggered widespread permafrost warming and degradation. Globally, permafrost temperature has increased by 0.29 ± 0.12°C between 2007 and 2016 (Biskaborn et al., 2019). The active layer thickness (depth of seasonally-thawed soil above permanently frozen material) in permafrost regions has deepened (Peng et al., 2018), and abrupt permafrost collapse or thermo-erosion (i.e. thermokarst) is increasingly occurring in areas with rich ground ice (Olefeldt et al., 2016; Turetsky et al., 2020). These changes are profoundly restructuring hydrological and ecological processes in permafrost regions (Vaks et al., 2020; Wang et al., 2020), with uncertain consequences for net ecosystem carbon balance and other ecosystem processes, such as vegetation change and lateral flux of material through rivers (McGuire et al., 2018; Shogren et al., 2019; Vonk et al., 2019).

On a basic level, the fate of permafrost organic matter depends on the amount of material thawed and the physical and biogeochemical conditions after thaw (Coolen et al., 2011; Schuur et al., 2015). More specifically, greenhouse gas production and consumption will depend on the interaction among the rate of permafrost degradation, the reactivity of thawed organic matter, the biochemical context after a thaw, other disturbance types, and ecosystem recovery trajectories (Egelkraut et al., 2018; Keuper et al., 2020; Lawrence et al., 2015; Li et al., 2020; Mack et al., 2011; Mack et al., 2004; Schädel et al., 2014; Shogren et al., 2019). While all these factors remain uncertain at the vast spatial scale of the permafrost zone (Metcalfe et al., 2018; Voigt et al., 2020), several key unknowns have been identified over the past decade, including 1) The evolution of moisture and nutrient conditions, which regulate the amount and type of greenhouse gases produced; 2) The type and extent of disturbance, such as thermokarst, wildfire, grazing, extreme hydrological events, and resource extraction, which can abruptly destabilize permafrost organic matter; and 3) Net greenhouse gas balance throughout the year, including the non-growing season (Abbott et al., 2016; Gentsch et al., 2018; McGuire et al., 2018; Natali et al., 2019; Schuur et al., 2015).

Controlled incubations and some ecosystem-level studies show net carbon release from thawed permafrost, on the order of 5 to 75% loss on decadal to centennial time scales (Elberling et al., 2013; Schuur et al., 2015). However, our incomplete understanding of the complexity of ecosystem response to permafrost degradation has resulted in projections of the net permafrost climate feedback that do not agree in magnitude or even direction (i.e., net greenhouse gas release or uptake) (Abbott et al., 2016; McGuire et al., 2018; Turetsky et al., 2020). Generating new process and scaling knowledge is exceedingly urgent to constrain this potentially extensive ecosystem feedback to anthropogenic greenhouse gas emissions.

In this paper, we synthesize the rapidly growing literature on permafrost and organic matter on the TP. Specifically, we present the 1) Permafrost status, including active-layer depth and multiple disturbance types; 2) Permafrost carbon storage; 3) Organic matter decomposition and ecosystem fluxes; and 4) Thermokarst landforms and their effect on the carbon cycle. Our objective was to improve understanding of the unique and general aspects of permafrost carbon dynamics in this region, which provide a valuable comparison to other permafrost regions globally. Additionally, we aim to provide an important baseline for future Earth-system studies by synthesizing the current research on TP permafrost carbon across many sites and study types. We hope this synthesis will contribute to better integration of TP and circumarctic research, including a greater understanding of regional consequences of change and global estimates of the permafrost climate feedback. The findings shall help policymakers about the management of permafrost landscapes including questions of soil carbon storage and ecosystem stability in these rapidly changing landscapes.

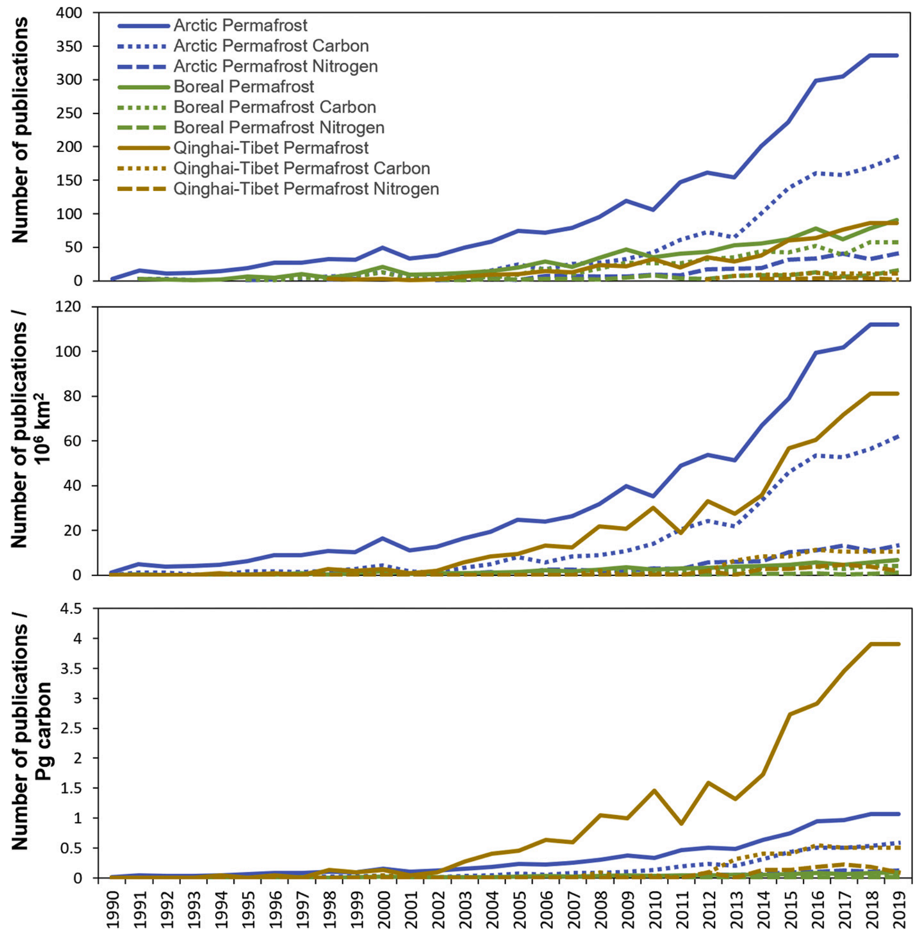

Fig. 2. Number of publications through time for various search terms associated with permafrost, carbon, and nitrogen. The first plot shows the overall number of publications. The second plot shows the publications divided by the surface area of the three regions. The third plot shows the publications divided by the organic carbon pools (vegetation plus SOC) of the regions.

1.1. Trends in permafrost research across regions

The number of permafrost-related articles in peer-reviewed journals has increased rapidly during the past decades both in the circumarctic (i.e. Arctic and Boreal biomes) and TP regions. To provide context on the relative research activity concerning Arctic, Boreal, and TP permafrost, we performed a meta-analysis on Web of Science (Clarivate Analytics). We performed the search in July of 2020 using the "topic" categorical search function. We extracted yearly publication counts for the last three decades of research, in addition to the all-time publication count and year of first mention. For all searches, we used the region name (Arctic, Boreal, or Qinghai-Tibet) and the word "permafrost." Because there are numerous names for the TP, we compared several permutations of the region name (i.e. "Tibet," "Tibetan," "Qinghai-Tibet"), and found similar results. We added the words "carbon" and "nitrogen" to the search to assess element-specific trends. In addition to the raw publication counts, we normalized the number of publications to the area and organic carbon content of each region. Web of Science states that its database extends from 1945 to 2020, which may truncate some of the years of first publication. While we recognize that this exercise does not comprehensively capture all the studies on this topic, it provides an internally consistent comparison among these regions.

We found that "Arctic permafrost" returned the most hits by far, followed by "Arctic permafrost carbon" and "Boreal permafrost" (Fig. 1). For all three regions, there were more hits for "carbon" than for "nitrogen", and the "nitrogen" first publication dates were later. Searches including "Qinghai-Tibet" returned fewer publications and the first publication dates were more recent.

The trends of publications through time confirmed the pattern of Arctic domination for the overall number of publications, including when normalized by area (i.e., there are not only the most studies overall on the Arctic, there are also the most per square kilometer; Fig. 2). However, when normalized to SOC stocks, the TP permafrost had the most publications per Pg, while the Boreal region had the least. We note that many studies use the term "Arctic" in a generic sense and that many of these studies likely include Arctic and Boreal research. Across all three regions, "nitrogen" continues to be underrepresented in the literature.

This simple analysis shows the rapid growth of research on the TP, which was severely underrepresented in the literature just a few decades ago, but which now has a similar number of studies per square kilometer and per Pg of organic carbon as the Arctic and Boreal regions (Fig. 2). This reflects the tremendous impact of the TP on the Asian and global climate (Li et al., 2018b) as well as its role as the water tower of east and south-east Asia (Cheng et al., 2019). Both the climatic and water security importance of this region is strongly affected by changing permafrost dynamics. However, the rapid growth of research on the TP highlights two continuing issues. First, there is a lack of synthesis work on the TP compared to the Arctic and Boreal biomes, where there are multiple, definitive syntheses and meta-analyses (Schuur et al., 2015; Strauss et al., 2017; Treat et al., 2015). Second, the research from the TP continues to be separated from Arctic and Boreal research (e.g., it is not well cited or integrated into conceptual models). For example, many of the permafrost syntheses cited previously do not include research from the TP, or at best mention the region briefly (Metcalfe et al., 2018; Moon et al., 2019; Natali et al., 2019; Schuur et al., 2015; Tank et al., 2020;

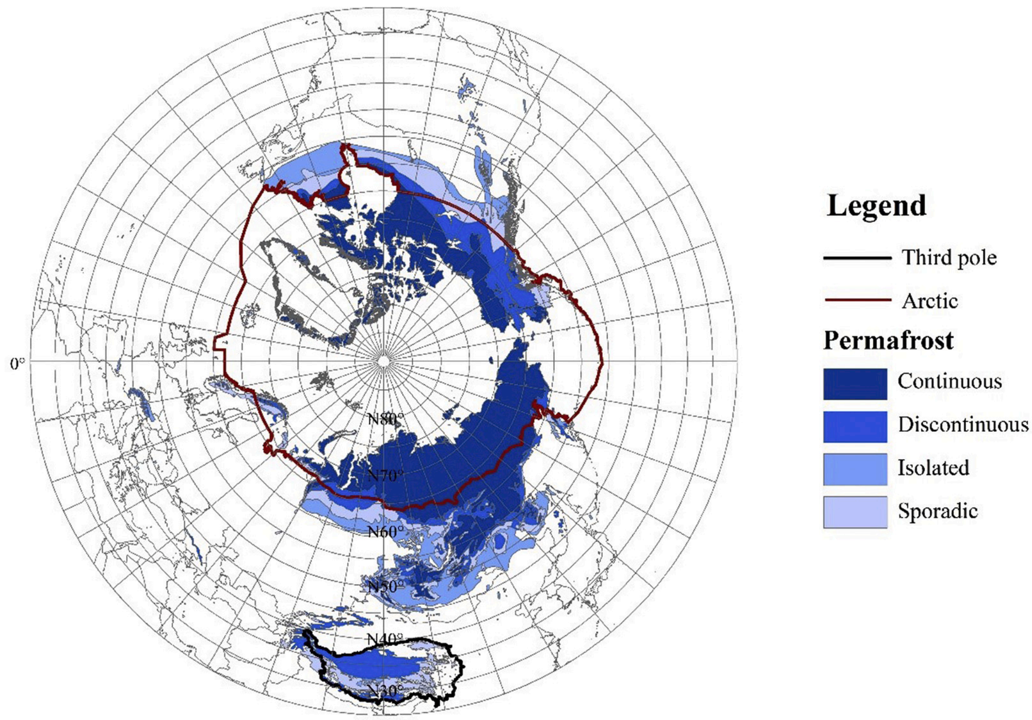

Fig. 3. Distribution of permafrost in the Northern Hemisphere, including Arctic and Boreal regions and the Tibetan Plateau or "Third Pole" (TP). The permafrost extent data were obtained from the National Snow & Ice Data Center (Brown et al., 2002). The Arctic area labeled is from the Arctic Monitoring & Assessment Programme (AMAP, 2019).

Turetsky et al., 2020). This geographic isolation represents a serious missed opportunity, as much of the new research from the TP applies to regions of the circumarctic and *vice versa*. More generally, this highlights the importance of synthesizing TP work into continental-scale estimates. Multiple syntheses are needed to better integrate ecosystem matter stocks and fluxes on the TP into global ecosystem budgets (Ding et al., 2016b; McGuire et al., 2018; Qin et al., 2019; Yang et al., 2019; Zhang et al., 2019c). Additionally, comparisons among regions of SOC stability and ecosystem recovery trajectories are needed to constrain the overall permafrost climate feedback. Overcoming these geographic siloes will require enhanced collaboration among teams working on the TP and also inter-regional collaborations, including Arctic, Boreal, and TP researchers.

1.2. Situating the Tibetan Plateau in a global permafrost context

Alpine permafrost underlies 3.6 to 5.2 million km^2, accounting for about 28% of the global permafrost area (Bockheim and Munroe, 2014; Hock et al., 2019; Obu et al., 2019). Alpine permafrost areas are mainly in the circumarctic, but they occur on every continent except Australia, including the European Alps, Scandinavia, Canada, High Mountain Asia, and North Asia. With an average height of over 4,000 m, the Tibetan Plateau (TP) and its surroundings in China are also known as the world's "Third Pole." The TP accounts for more than half of the alpine permafrost area outside of the circumarctic (Yang et al., 2019), with an area underlain by permafrost of approximately 1.06×10^6 km^2 (Fig. 3). The TP plays an important role in the stability of Asia's climate system, water supply, biodiversity, and regional carbon balance, making it indispensable to global biosphere integrity and sustainable development of surrounding areas (Kang et al., 2019). On the TP, permafrost exerts direct controls on the availability and quality of fresh water, with consequences for billions of humans and many ecosystems (Cheng et al., 2019). Synthesizing existing research about permafrost and organic matter on the TP is therefore crucial for local and global reasons (Jin et al., 2007).

Permafrost warming and degradation, including ground temperature increase and active layer thickness (ALT) deepening, have been widely recorded on the TP (Cao et al., 2018; Wu et al., 2015; Wu et al., 2010). These changes are already affecting regional carbon, nutrient, and water cycles (Yang et al., 2019; Zhao et al., 2018). In addition to direct climate warming, disturbance such as wildfires (Schmitz et al., 2014) and grazing (Väisänen et al., 2014) can also affect SOC dynamics in many permafrost regions (Carey et al., 2019; Egelkraut et al., 2018; Kirdyanov et al., 2020). Currently, there is almost no wildfire reported on the TP, and grazing has affected some soil properties (Hopping et al., 2018), livestock and human densitiyis low due to the national environmental protection policies, resulting in limited impacts (Yuan et al., 2020). In contrast with these disturbances, thermokarst formation has been recognized as an important factor influencing net ecosystem carbon balance and ecosystem greenhouse gas emissions on the TP (Liu et al., 2018a; Mu et al., 2017c). Thermokarst landscapes, such as thaw slumps and thermokarst lakes, significantly affect SOC stocks and fluxes through a range of soil erosion and deposition processes (Mu et al., 2016c; Wu et al., 2018 Wu et al., 2018b). These landform changes suggest that soil carbon will likely experience rapid loss in addition to being transported laterally as dissolved organic carbon (DOC) (Gao et al., 2019;) and particulate organic carbon (POC) through surface-water networks and the sea (Abbott et al., 2018; Tank et al., 2020). Although thermokarst features on the TP have attracted wide attention due to their evident and severe impacts on ecology and infrastructure (Niu et al., 2005), the landscape-level importance of these features is not agreed upon by different research teams on the TP (Niu et al., 2005; Wu and Zhang, 2010).

2. Responses of permafrost to climate change

2.1. Climate change

The warming rate of the TP is more than twice the global average in the past 50 years, similar to rates of warming in the Arctic (Kuang and

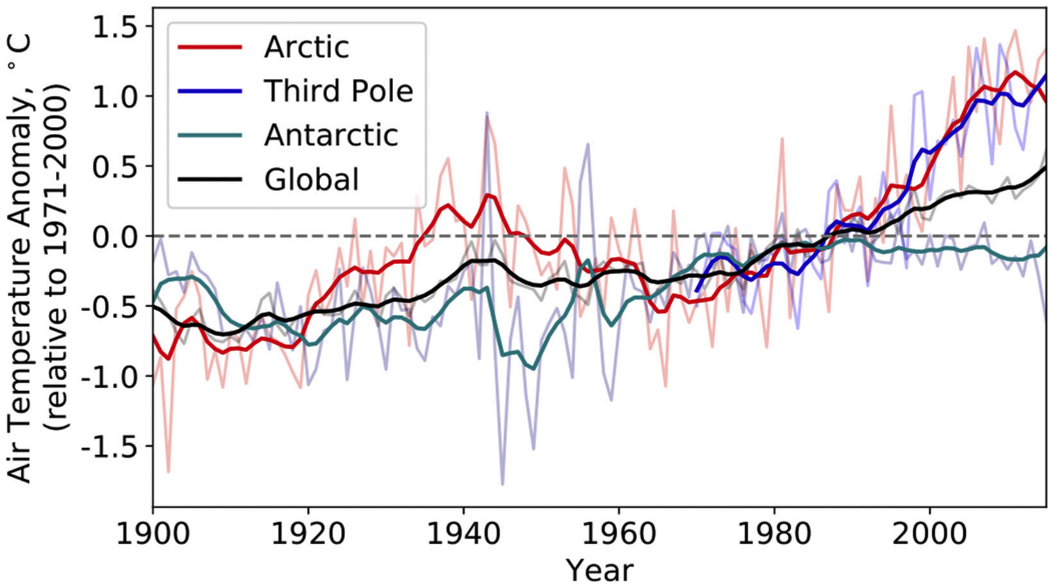

Fig. 4. The Tibetan Plateau, Arctic, Antarctic, and global annual surface air temperature anomalies relative to the 1971–2000 mean value. For the Tibetan Plateau, data are obtained from the ground-based stations derived by China Meteorological Administration. Data for global, Arctic, and Antarctic are obtained from the NOAA/GLOBALTEMP dataset. Thin lines are annual mean surface temperature anomalies and thick ones are their corresponding low pass filter lines with a cut-off frequency of 0.091.

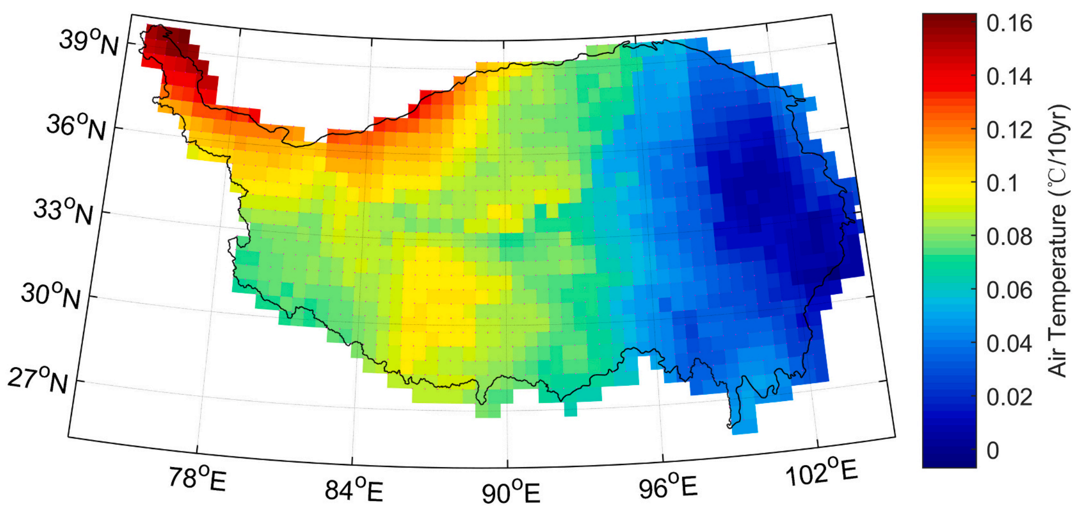

Fig. 5. Spatial variation in trends of mean annual air temperature on the Tibetan Plateau during 1901–2018. The figure was created using the data from the Climatic Research Unit time-series v. 4.03, developed by the University of East Anglia (http://www.cru.uea.ac.uk/), with a spatial resolution of 0.5°× 0.5°.

Jiao, 2016; Pang et al., 2012; Yang et al., 2019) (Fig. 4). However, there are large spatial heterogeneities in the air temperature increase on the TP (Fig. 5), with the fastest warming in the northwest and the slowest in the east (Guo et al., 2012; Wang et al., 2014). Long-term warming has been observed across all seasons, though wintertime warming has been the most extreme (Wang et al., 2014). In winter, the air temperature has increased at a rate of 0.66°C per decade from the 1980s to the 2000s, which is almost double the average summer warming rate (Zhang et al., 2019a). Although the precipitation change over the TP is complex and has regional differences (Yang et al., 2019), the precipitation for the whole TP increased at a rate of 3.1~5.1 mm per decade from the 1960s to the 2010s (Chen et al., 2013; Kang et al., 2010; Wang et al., 2018a).

2.2. Ground temperature and active layer thickness

The significant changes in air temperature and precipitation on the TP described above have warmed permafrost, threatening its stability and persistence (Ding et al., 2019b; Yang et al., 2019). TP permafrost has a relatively warm temperature, typically within a few degrees below the freezing point (Wu and Zhang, 2008). The mean annual ground temperature (MAGT) is defined as the temperature at a depth of zero annual amplitude, where the amplitude of annual average ground temperature change is less than 0.1°C. Stable permafrost (-3°C<MAGT<−1.5°C) accounts for 30.4% of the total TP permafrost area, while transitional permafrost (-1.5°C<MAGT<−0.5°C) and unstable permafrost (-0.5°C<MAGT<0.5°C) both account for 22.6% (Cheng et al., 2019). Based on 18 deep boreholes in the permafrost regions of the TP (Fig. 6), the average warming rate of ground temperature at a depth of 10 m along the Qinghai-Tibet Highway was 0.14°C per decade from 2003–2015 (Fig. 7) (Zhang et al., 2019a). Observations over the Heihe River basin of the Qilian Mountains in the northern TP (Cao et al., 2018) showed that the MAGT at a depth of 16 m increased at a rate of about 0.48°C per decade from 2012–2019 (Fig. 7). This warming rate is similar to those in Fenno-Scandinavia and the western Siberian Arctic, where the temperatures at 10 m depth for cold permafrost sites have increased by 0.4–0.6°C per decade since the late 1980s (AMAP, 2017). The ground temperature rate of increase is higher than continuous permafrost zones at a global scale, where the ground temperature warmed by 0.39 ± 0.15°C from 2007–2016 (Biskaborn et al., 2019).

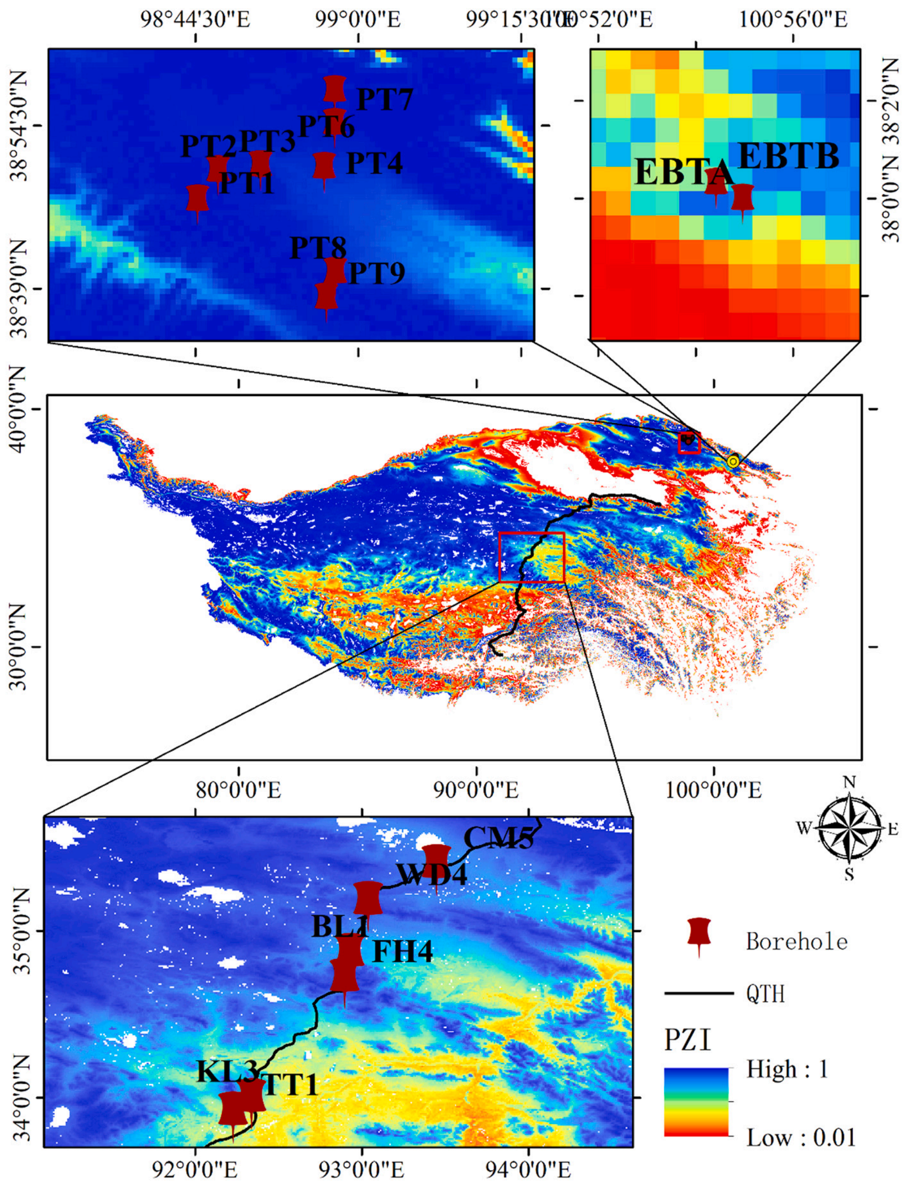

Fig. 6. Locations of 18 deep boreholes for permafrost temperature monitoring along the Qinghai-Tibet Highway (boreholes of BL1, TT1, KL3, CM5, FH4, and WD4) and over the Heihe River Basin of Qilian Mountains (boreholes of PT1-PT4, PT6-PT9, EboTA, and EboTB) in the Tibetan Plateau. The background map shows the high-resolution permafrost zonation index (PZI), indicating the likelihood of permafrost presence, with the red color indicating permafrost only exists under the most favorable local conditions, and the blue color indicating continuous permafrost (Cao et al., 2019).

The active layer thickness (ALT) of the TP permafrost is deep by permafrost standards (Qin et al., 2017). The ALT is estimated as the maximum thaw depth in the late autumn through linear interpolation of soil temperature profiles between two neighboring points above and below the 0°C isotherm (Burn, 1998). Currently, the ALT on the TP ranges from 100 to 400 cm, with an average value of approximately 220 cm (Cao et al., 2019). Through field monitoring, a previous report suggested that the average ALT along the Qinghai-Tibet Highway increased 7.5 cm/a from 1995 to 2007 (Wu and Zhang, 2010). A recent report showed that ALT along the Qinghai-Tibet Highway increased at a much higher rate of 21.7 cm per decade from 2004 to 2018 (Zhao et al., 2019). The large difference between these estimates is explained by the fact that that these results were obtained from different sites with considerable heterogeneity in permafrost and soil properties (Loranty et al., 2018). Based on the relationship between meteorological data and ALT, a regression analysis showed that the average ALT along the Qinghai-Tibet highway from 1981 to 2010 increased by 13.3 cm per decade (Li et al., 2012), and the ALT along the Qinghai-Tibet Highway increased by 19.5 cm per decade from 1982 to 2018 (Zhao et al., 2019).

In addition to increasing ALT, the soil temperature in the active layer also shows increasing trends on the TP. Based on observed and reanalysed meteorological data from the European Centre for Medium-Range Weather Forecasts-interim reanalysis, the rate of annual mean soil temperature warming from 1980 to 2015 in the active layer was 0.44°C per decade for 0–10 cm, 0.45°C per decade for 10–40 cm, 0.40°C per decade for 40-100 cm, and 0.26°C per decade for 100–200 cm (Hu et al., 2019).

All the field monitoring and modeling results clearly indicated that the MAGT, ALT, and soil temperature in the active layer significantly increased over the TP. However, the spatial distribution of field monitoring sites is very uneven, and there are great spatial heterogeneities in the MAGT and ALT, making it challenging to obtain conclusive information about permafrost degradation for the whole TP.

2.3. Thermokarst development

The warming of permafrost and deepening of the active layer in ice-rich permafrost regions of the TP have resulted in widespread thermokarst formation that includes thaw slumps, thermal erosion, and thermokarst lakes (Mu et al., 2017c; Niu et al., 2012). These dynamic thermokarst processes can affect sloping and flat terrain overlaying ice-rich permafrost (Jorgenson and Osterkamp, 2005; Kokelj and Jorgenson,

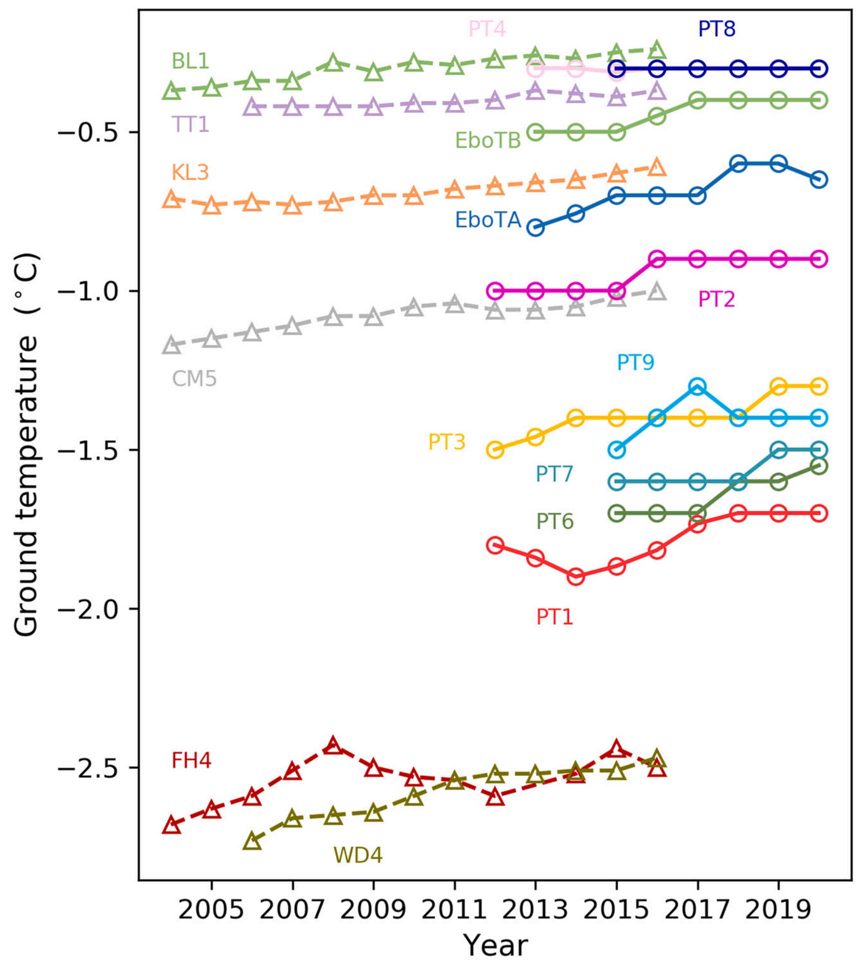

Fig. 7. Changes of ground temperature for the 18 permafrost boreholes along the Qinghai-Tibet Highway (the depth of ground temperature for boreholes of BL1, TT1, KL3, CM5, FH4, and WD4 is 10 m) and over the Heihe River Basin of Qilian Mountains (the depth of ground temperature for boreholes of PT1-PT4, PT6-PT9, EboTA, and EboTB is 16 m). The data of ground temperatures were retrieved from the follwing publications (Cao et al., 2018; Zhang et al., 2019a).

2013). Thermokarst formation can rapidly expose and thaw thick layers of underground ice or ice-rich permafrost, modify land surface morphology, and transport large volumes of thawed materials laterally downslope or downstream (Kokelj and Jorgenson, 2013; Weege et al., 2014). These features are very diverse, with many of them not falling neatly within typical morphological categories (Abbott et al., 2015b; Kokelj and Jorgenson, 2013). Common forms on the TP include elongated thaw slumps resembling active-layer detachments and thermo-erosional gullies (Huang et al., 2020; Luo et al., 2019; Mu et al., 2020b) (Fig. 8). Different morphologies are common in alpine meadow, wet meadow, and desert steppe, depending on the ground ice content, slope, soil properties, and hydrology (Mu et al., 2020a; Mu et al., 2020b). In the eastern TP, which has land cover types of meadow and wet meadow, permafrost collapse can result in deep pits with a depth of ~6 m (Fig. 8a, b). In the central TP, which has an alpine desert steppe land cover, thermokarst terrains are usually manifested as retrogressive thaw slumps (Fig. 8c, d). These thaw slumps are also common in eastern regions but are rare in the west where the climate is dry and the ground ice content is low (Cheng et al., 2019).

Unlike the circumarctic (Olefeldt et al., 2016), there is currently not an estimate of the total thermokarst-affected area on the TP. However, several regional estimates demonstrate an increase in thermokarst on the TP due to climate change and disturbance from construction (e.g., roads, pipelines, and buildings) over the past few decades (Luo et al., 2019; Niu et al., 2014; Sun et al., 2017; Wang et al., 2018b). Due to remoteness and technical challenges of automatic mapping based on remotely sensed data (Balser et al., 2014), the spatial distribution and effects of thaw slumps on the TP are not well constrained. Recently, Unmanned Aerial Vehicle (UAV) images have been used to detect thermo-erosion landforms on the Northeastern TP, with 16 thermo-erosion gullies detected in an area of 6 km^2 (Fig. 9) (Huang et al., 2018). Based on field investigation and deep learning (a cutting-edge algorithm for semantic segmentation), 220 thaw slumps were identified within an area of 5,200 km^2 in the central TP (Fig. 9) (Huang et al., 2020). Using a series of satellite images from 2008 to 2017, including Gaofen-1, WorldView-I, and Panchromatic SPOT-5 images, it was shown that the total number of thaw slumps increased from 124 to 438 over that time period, and the total affected area increased from 1.31 km^2 to 9.34 km^2 within the ~3,700 km^2 Beilu River Basin (Luo et al., 2019). The acceleration of thaw slump development is mainly attributed to increasing air temperatures and precipitation during the thawing season. Like for the circumarctic (Turetsky et al., 2020), much work is still needed to catalogue thermokarst formation and upscale its ecosystem consequences, as the areal extent of thermokarst features likely greatly exceeds the observed extent of active features (Balser et al., 2014; Bowden et al., 2008; Farquharson et al., 2019; Tanski et al., 2017).

Thermokarst lakes are formed due to ground settlement triggered by the melt of ground ice (Jorgenson et al., 2008). These lakes play an important role in the accumulation of organic matter and release of greenhouse gases, particularly of methane (Anthony et al., 2014; In't Zandt et al., 2020). The distribution of thermokarst lakes is closely related to permafrost characteristics such as ice content and ground temperature. In the Northern Hemisphere, thermokarst lakes are the most apparent feature of permafrost degradation, occupying 20–50% of

Fig. 8. Field pictures showing thaw slumps, gullies, and active-layer detachments in alpine meadow and wet meadow in the Northeastern area (Eboling Mountain, a, b) and in the alpine desert steppe in the central area (Beilu River basin, c, d) of the Tibetan Plateau.

permafrost-affected landscapes (Grosse et al., 2008; Hinkel et al., 2007; Zhang and Zhong, 2014). Based on long-term observations from 1970 to 2013 (Zhang et al., 2017a), approximately 150,000 lakes (>1000 m^2) are distributed in the permafrost regions of the TP (Fig. 10). The total area of lakes in the permafrost regions is approximately 2.9×10^4 km^2, which represents about 2.7% of the total permafrost area on the TP. Presently, it is difficult to identify which of these lakes are thermokarst lakes, and many small thermokarst lakes and ponds were not included in this dataset. A high-quality dataset for thermokarst lakes on the TP using observation data and numerical model would be helpful for further research on the changes in the ecological environment of the TP.

Recent climate warming has accelerated the development of thermokarst lakes on the TP (Luo et al., 2015). Small water pits may develop into thermokarst lakes after undergoing sustained slumping and collapse. In a study area of 2,510 km^2 in the Beilu River Basin of the central TP, aerial and satellite images from 1969, 2003, and 2010 showed that the number of thermokarst lakes increased from 761 to 1,295 and the total lake area increased from 32.4 km^2 to 36.4 km^2 (Luo et al., 2015). The number of small lakes increased, and the areas of large lakes expanded (Luo et al., 2015). We note that the development of thermokarst lakes on the TP may follow different trajectories than in the circumarctic. Arctic and Boreal permafrost typically has a thinner active layer and lower ground temperature compared to the TP, thus there are generally small taliks (permanently thawed pockets of sediment within the permafrost) under thermokarst lakes (Hinkel et al., 2012). Observations from drilling have indicated that contiguous taliks often form under thermokarst lakes on the TP (Ling et al., 2012; Ling and Zhang, 2018). This can result in either the expansion or draining of lakes, depending on the hydraulic conductivity in thawed substrate (Nitze et al., 2017).

3. Permafrost carbon pools on the TP

3.1. Distribution of land-cover types

Vegetation plays a crucial role in carbon cycling and the permafrost thermal state (Loranty et al., 2018; Shur and Jorgenson, 2007), making it a useful proxy for estimating permafrost presence and ecosystem carbon stocks (Jiang et al., 2018; Wang et al., 2002). Consequently, the accuracy of land cover type distribution data will greatly affect estimates of soil carbon. A vegetation map of the TP was created in 2001 (1:1,000,000, Editorial board of vegetation map of China CAS, 2001) (Yu et al., 2010; Zhang et al., 2013), which included alpine meadow, alpine desert, and alpine steppe. This map has been widely used for the estimation of permafrost carbon storage (Yang et al., 2010; Yang et al., 2008). However, this dataset did not include the alpine wet meadow and barren land, which are very distinct from other land cover types in regard to carbon storage. In addition, the vegetative area in the TP has been expanding, and vegetation growth has also been increasing due to the climate change (Mu et al., 2015; Piao et al., 2012; Zhang et al., 2013). Therefore, it is important to create a detailed and updated map of the land cover in the permafrost zone of the TP. In 2016, a principal component analysis and decision tree classification algorithm was used to map the land cover type distribution on the TP based on remotely-sensed data and 490 ground truthing vegetation sampling sites (Wang et al., 2016). This resulted in the classification of four land cover types–alpine wet meadow, alpine meadow, alpine steppe and desert—covering approximately 4.2%, 48.6%, 27.7%, and 19.5% of the TP permafrost area, respectively. In addition to these vegetated areas of 1,201,751 km^2, there is a large permafrost area of barren land, with an area of 282,657 km^2 (Wang et al., 2016). Neglecting this barren land could lead to overestimation of total SOC storage of the TP permafrost area because it has a much lower SOC stock than other land cover types (Zhao et al., 2018).

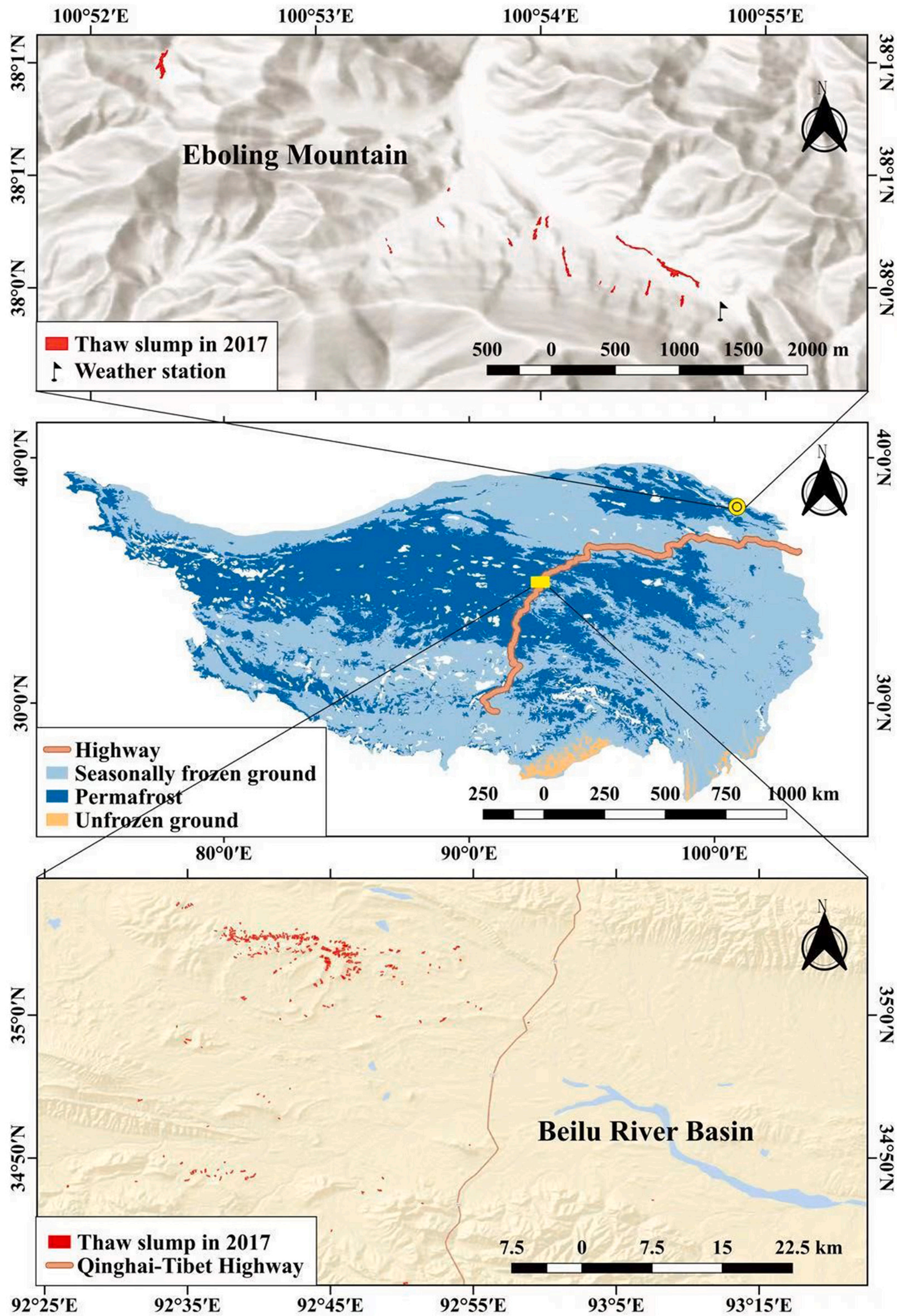

Fig. 9. Distribution of thaw slumps in the Eboling Mountains (Huang et al., 2018) and the Beilu River Basin (Huang et al., 2020).

3.2. Distribution of SOC and its controlling factors

The SOC stocks on the TP show great variability in their horizontal and vertical distributions. Horizontally, the stocks of SOC decrease from the southeastern to the northwestern areas of the TP, related to precipitation and the influence of the southern tropical and eastern subtropical monsoons (Baumann et al., 2009b; Jiang et al., 2018; Yang et al., 2008). This pattern of SOC decrease is closely associated with the land cover types, i.e., the SOC stocks showed the highest values in the alpine wet meadow, followed by the alpine meadow and steppe, and finally the desert steppe and barren land with the lowest values (Liu et al., 2012;). Vertically, SOC content is concentrated in the surface soil and decreases exponentially with depth (Du and Gao, 2020; Hu et al., 2014; Liu et al., 2012; Wu et al., 2012). Consequently, the uppermost 50 cm of soil contains 36-50% of the total SOC stocks from 0 to 300 cm (Ding et al., 2016b). Some areas with higher SOC contents also exist at

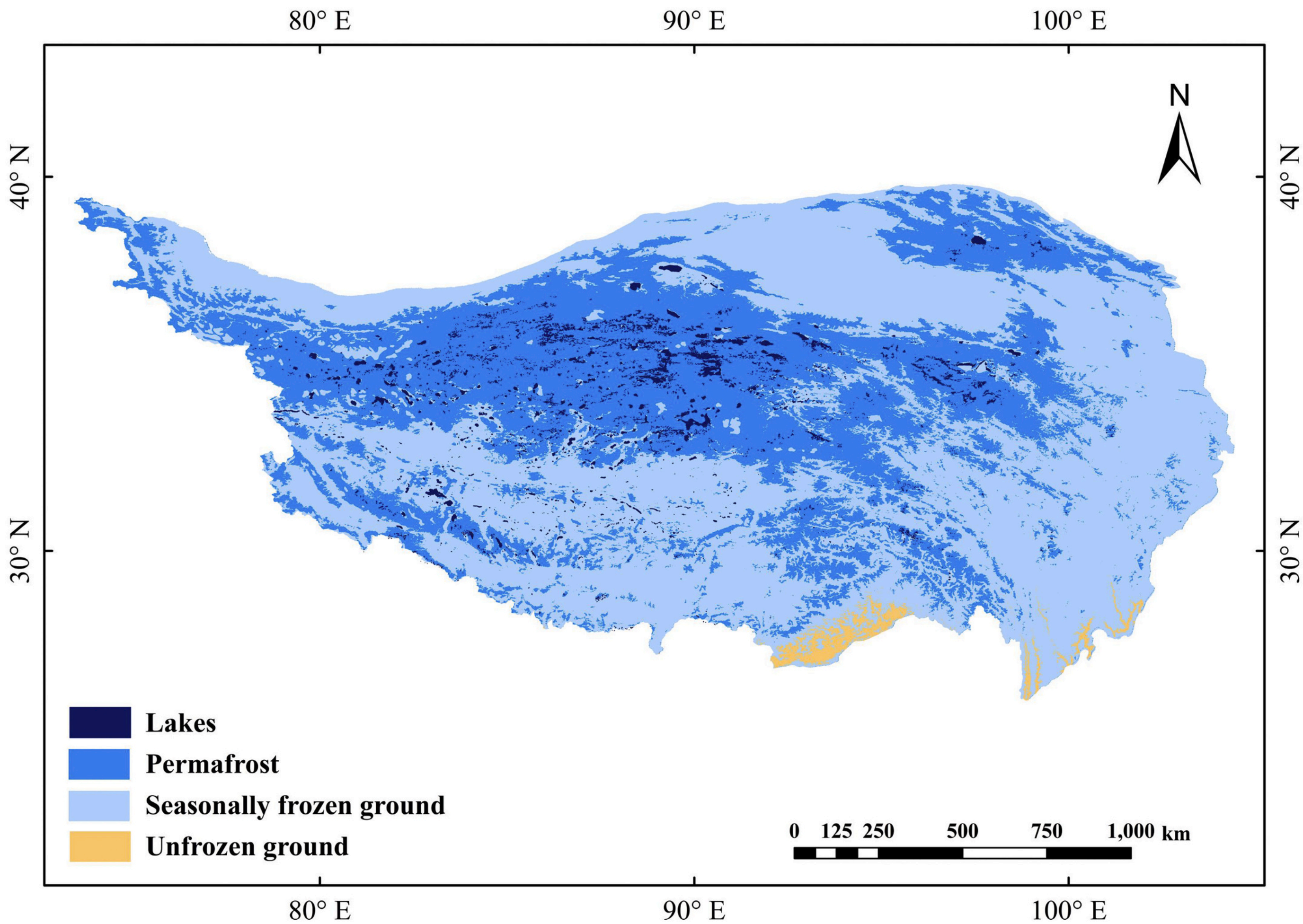

Fig. 10. Spatial distribution of lakes (>1,000 m^2) (Zhang et al., 2017a) in the permafrost and non-permafrost regions (Zou et al., 2017) of the TP.

the bottom of the active layer and into permafrost layers, due to the cryoturbation and sediment burying process (Bockheim, 2007; Ping et al., 2008b).

Many factors such as land cover type, soil water content, soil texture, pH, and active layer thickness are correlated with SOC stocks (Baumann et al., 2009b; Hu et al., 2014; Liu et al., 2012; Wu et al., 2012; Yang et al., 2008). It is well known that land cover types affect SOC content because it mainly originates from products that develop from dead plants and animals that decompose and the soil microbial biomass. Therefore, the large differences in above-ground and below-ground

Table 1
Recent estimates of soil carbon pools for 0-3 m depth in the permafrost region of the Tibetan Plateau

Data sources	Calculation methods	Estimated permafrost area (10^4 km^2)	Vegetation with area (10^4 km^2)	SOC stocks (kg C m^{-2})			SOC storage (Pg)			References
				0-1 m	0-2 m	0-3 m	0-1 m	0-2 m	0-3 m	
190 soil profiles through field sampling	Upscaling with vegetation types and geological stratigraphies	124.9	AM (30.2)	—	—	—	11.3	16.4	18.4	(Mu et al., 2015)
			AS (77.2)	6.9	13.4	23.0	5.3	10.3	12.6	
			AD (17.5)	3.8	6.8	12.4	0.7	1.2	2.0	
			Total	—	—	—	17.3	27.9	33.0	
342 3-m-depth cores and 177 0.5-m-depth pits through field sampling	Machine learning technique	114.4	AS (64.0)	4.5	6.6	8.6	2.9	4.2	5.5	(Ding et al., 2016b)
			AM (45.3)	9.0	12.0	14.4	4.1	5.4	6.5	
			SM (5.1)	30.8	51.3	65.0	1.6	2.6	3.3	
			Total	7.4	10.7	13.4	8.5	12.2	15.3	
200 soil pits through field sampling	Upscaling with vegetation distributions	148.4	AWM (5.0)	38.3	53.0	—	1.9	2.7	—	(Zhao et al., 2018)
			AM (58.4)	14.1	17.5	—	7.4	8.8	—	
			AS (33.3)	5.5	7.7	—	1.8	2.6	—	
			AD (23.5)	3.9	7.4	—	0.9	1.7	—	
			BL (28.3)	2.4	4.7	—	0.7	1.3	—	
			Total	64.2	90.2	—	12.7	17.1	—	
China's second national soil survey in 1980s	Upscaling with soil classification	158.8	Total	11.2	—	25.8	17.8	—	40.9	(Jiang et al., 2018)
314 sites from literatures	Machine learning technique	130.0	Total	—	—	—	—	—	15.33	(Wang et al., 2020)

AM: alpine meadow, AS: alpine steppe, AD: Alpine desert, AWM: alpine wet meadow, BL: barren land.

biomass and soil microbial communities among different land cover types strongly influence SOC accumulation (Liu et al., 2018a; Mu et al., 2018; Wild et al., 2014). Soil water content, soil texture, and pH are factors affecting soil organic matter decomposition rates via microbial and abiotic (e.g. sorption of SOC to reactive soil minerals) stabilization mechanisms (Giardina and Ryan, 2000). The ALT can affect SOC accumulation rates because areas with a shallow active layer have a low soil temperature and cryoturbation process that mix SOC deeper into the profile (Bockheim and Munroe, 2014), both slowing down decomposition rates of SOC. Low soil temperature can inhibit microbial production of greenhouse gases and cryoturbation can bring organic-rich soil from the surface into deeper layers (Ping et al., 2008b). In the eastern TP, the shallower ALT usually corresponds with higher SOC contents though this is not the case in the western TP regions where permafrost is either too deep (i.e., ALT includes most or all SOC) or too dry to affect carbon accumulation (Wu et al., 2016).

As for many circumpolar permafrost regions (Abbott et al., 2015b; Malone et al., 2018; Rasmussen et al., 2018), SOC on the TP is related to multiple factors via complex, and sometimes nonlinear interactions (Baumann et al., 2009a; Dorfer et al., 2013; Hu et al., 2014; Liu et al., 2021). For example, low bulk density is usually associated with fine soil particle size, which has high soil water holding capacity. The high soil water content is associated with high above-ground and below-ground biomass, and shallow ALT (Hu et al., 2014). These conditions favor the accumulation and preservation of SOC (Liu et al., 2012). Based on data from 73 soil pedons, it was found that SOC stocks are primarily controlled by the soil particle size distribution in the permafrost regions on the TP (Wu et al., 2017a). However, these relationships are often scale dependent. For example, at the site scale, SOC content is mainly associated with soil texture and soil water content (Hu et al., 2014; Wu et al., 2017a). At the plateau scale, the SOC content correlates with land cover types and climate, which are associated with the geographical location such as longitude and latitude (Zhao et al., 2018). At the regional scale, the TP has highly varied topography characterized by rugged topographical conditions, such as deep valleys and high mountains. Topography can greatly affect land-cover types, micro-climatic conditions, pedogenesis, and permafrost distribution (Wu et al., 2018). Increasing the spatial resolution of SOC sampling across topography and ecosystem types would improve the estimation of carbon pools on the TP.

3.3. SOC stocks of the Tibetan Plateau

Presently, there are many independent estimates of SOC stocks for different ecosystem types on the TP permafrost region. Based on previously reported data (Table 1), alpine meadow and steppe are the dominant land-cover types on the TP. Average SOC stocks from 0–2 m depth are 14.4–17.5 kg m^{-2} for alpine meadow and 6.6–7.7 kg m^{-2} for alpine steppe. These SOC stocks on the TP permafrost region are substantially lower than in the North American Arctic (Canada and Alaska), where lowlands may have 55.1 ± 18.9 kg m^{-2} in the upper 1 m and uplands may have 40.6 ± 22.7 kg m^{-2} in the upper 1 m layer (Ping et al., 2008a). However, these stocks are somewhat closer to permafrost soils along a longitudinal gradient in the Siberian Arctic where there was 20.2 ± 8.0 kg m^{-2} in the upper 1 m (Gentsch et al., 2015).

Concerning overall SOC stocks for the TP, several studies have published estimates of the SOC pools in the grasslands for the whole TP (Ding et al., 2019a; Wang et al., 2002; Yang et al., 2010; Yang et al., 2008), while only four studies have estimated overall carbon pools in the TP permafrost regions (Table 1). Estimates of the 0–3 m SOC pool vary by a factor of 2.7, ranging from 15.3 Pg to 40.9 Pg in the TP permafrost regions. Based on 190 soil profiles in the TP permafrost regions, SOC storage within the estimated permafrost area of 124.9 × 10^4 km^2 was modeled using vegetation type and geological stratigraphies over the TP (Mu et al., 2015). From this analysis, the SOC pools in the permafrost regions were estimated to be 17.3 ± 5.3 Pg C for the 0-1 m depth, 10.6 ± 2.7 Pg C for the 1–2 m depth, and 5.1 ± 1.4 Pg C for the 2–3 m depth. (Mu et al., 2015). Based on the data from 342 3 m-depth cores and 177 0.5 m-depth pits, combined with the enhanced vegetation index dataset, and climatic and edaphic properties obtained using Kriging interpolations, support-vector regression was performed to estimate OC storage over a permafrost area of 1.14 × 10^6 km^2. The SOC pool was estimated to be approximately 8.5 Pg C for 0-1 m depth, 12.2 Pg C for the 0–2 m depth, and 15.3 Pg C for the upper 3 m of soil on the TP (Ding et al., 2016b). With the update of the vegetation map (including wet meadow and barren land in the permafrost zone) and 200 soil pits on the TP, the SOC pool was upscaled for the whole estimated permafrost area of 148.4 × 10^4 km^2; this study estimated that 12.7 Pg C is stored in 0-1 m layer and 17.1 Pg C in the upper 2 m soil layer (Zhao et al., 2018). According to the China's second national soil survey on the TP in the 1980s, SOC storage within the estimated permafrost area of 1.59 × 10^6 km^2 was estimated as 40.9 Pg C for the upper 3 m of soil on the TP (Jiang et al., 2018). This SOC storage in TP permafrost regions was distributed as 8.5–17.8 Pg for 0–1 m, 12.2-27.9 Pg for 0–2 m, and 15.3–40.9 Pg for 0–3 m (Fig. 11).

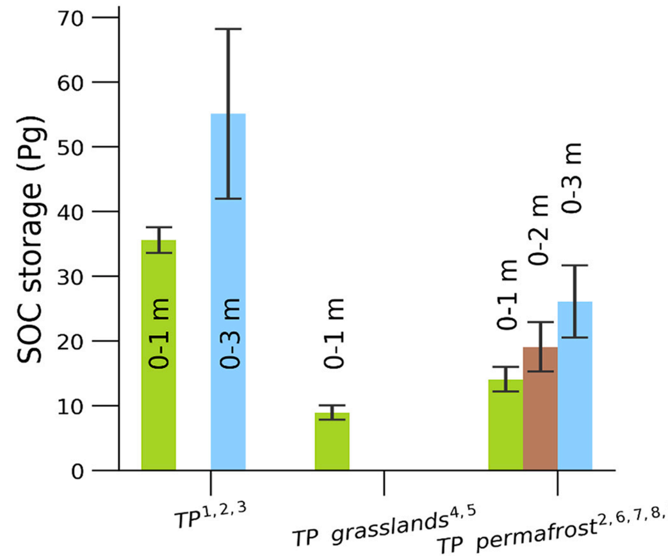

Fig. 11. Soil organic carbon (SOC) pools in the Tibetan Plateau permafrost regions. Inventories from 1, 2, 3 for the whole TP regions (Fang et al., 1996)[1], (Jiang et al., 2018)[2], (Ding et al., 2019a)[3], 4, 5 for the TP grasslands (Yang et al., 2010; Yang et al., 2007)[4,5], 2, 6, 7, 8 for the TP permafrost regions (Jiang et al., 2018)[2], (Ding et al., 2016b)[6], (Mu et al., 2015)[7], (Zhao et al., 2018)[8], (Wang et al., 2020)[9].

There are significant uncertainties in the SOC pools in the TP permafrost areas, stemming from both, differences in data sources and methods used for SOC estimation. First, although the TP area underlain by permafrost is about 1.06×10^6 km^2(Zou et al., 2017), the permafrost carbon pools include the SOC stored in some areas without permafrost in the discontinuous permafrost zones. The permafrost areas used in previous reports ranged from 1.14 ×10^6 km^2 to 1.59 ×10^6 km^2, which can lead to a direct difference in SOC estimates. Second, different vegetation and soil maps were used to calculate the SOC pools, making it difficult to compare these results. In addition, differences in the quantification methods for measuring SOC also contribute to the discrepancy in the SOC pools and content. Some data sources include China's second national soil survey on the TP, conducted in the 1980s, in which a set conversion factor of 0.58 (the Bemmelen index) was used to convert organic matter into organic carbon content. This conversion is quite different from the direct measurement of SOC content using elemental analysis.

Several calculation methods were used to extrapolate the TP permafrost SOC pools from somewhat limited SOC observations that are

Table 2
Responses of soil organic carbon (SOC) decomposition to short-term warming by aerobic incubation in the permafrost of the Tibetan Plateau and circumarctic regions.

	Land cover	Soil depth (m)	Incubation T (°C)	Incubation time	Mean Q_{10} values and ranges	Q_{10} estimation methods	References
Tibetan Plateau	AM, AS, DS	0 ~ 0.2	+4 to +28	2 h	2.9	Ramp of temperature	(Li et al., 2018a)
	AS, AM	0 ~ 0.1	+5 ~ +25	< 36 h	4.2	Ramp of temperature	(Ding et al., 2016b)
	AWM	0 ~ 1.1	-5 ~ +5	140 days	8.8	Ramp of temperature	(Mu et al., 2016b)
	ASM	1.5 ~ 4.0	-5 ~ +5	140 days	20.8	Ramp of temperature	(Mu et al., 2016b)
Arctic regions	BF	0.35 ~ 1.0	-5 ~ +5	98 days	2.3 ~ 2.7	Ramp of temperature	(Waldrop et al., 2010)
	Tundra, Shrub	0.2 ~ 1.7	+4 ~ +16	91 days	1.2 ~ 1.4	Ramp of temperature	(Moni et al., 2015)
	BF	40-120	+10 ~ +20	57 days	0.7 ~ 1.9	Long term parallel incubation	(Wickland and Neff, 2008)
	WM, IT, Tussock, Shrub	0 ~ 0.25	+0.5 ~ +14	183 days	4.9 ~ 9.4	Ramp of temperature	(Mikan et al., 2002)
	Tundra, BF	0.1-13.0	+5 ~ +15	90 days	1.7~2.9	Long term parallel incubation	(Dutta et al., 2006)

AM: Alpine Meadow, AS: Alpine Steppe, DS: Desert Steppe, ASM: Alpine wet meadow, WM: Wet meadow, IT: Intertussock, BF: Boreal forest. Ramp of temperature means the samples are submitted to increasing temperature.

distributed along highways and clumped in the eastern TP (Ding et al., 2016b; Mu et al., 2015; Zhao et al., 2018). Although there were accuracy assessments for these methods, the validation data were from different land cover and soil types. Thus it is difficult to compare the calculation methods among direct extrapolations using vegetation maps and multiple machine learning algorithms. Based on the three reports which used the most original data (Ding et al., 2016b; Mu et al., 2015; Zhao et al., 2018), the SOC pools for the 0–2 m soils were calculated as 19.0 ± 6.6 Pg, while the deep SOC pools remained largely unconstrained (15.3 to 40.9 Pg within 0-3 m depth). Because of the TP permafrost region's harsh natural conditions and sparsely populated area, fieldwork is challenging, especially deep borehole drilling. Therefore, regardless of what analytical advances are made in the near future, disagreement about deep SOC storage on the TP is likely to continue for several years, representing an important uncertainty in global carbon budgets and climate negotiations.

4. Vulnerability of permafrost carbon

4.1. Soil organic matter (SOM) decomposability

SOM decomposition in permafrost-affected soils is controlled by a complex interplay of environmental parameters such as substrate quality, soil temperature, water content, oxygen conditions, reactive minerals, nutrient availability, microbial abundance, and rhizosphere primers for co-metabolic decomposition (Chen et al., 2016; Hobbie et al., 2000; Keuper et al., 2020; Li et al., 2018a; Rasmussen et al., 2018; Xu et al., 2018). The lability or decomposability of SOM influences how much carbon stored in soil reservoirs can be mineralized to the atmosphere after thawing. Because SOM is a complex mixture of substances having different turnover rates, three conceptual carbon pools have been classified: an active pool containing the components of fresh plant litter with turn over times ranging from 20 to 70 years; a slow pool with turnover times in the range of years to centuries; and a passive pool of stabilized organic matter that persists in soils over thousands of years (Torn et al., 1997; Trumbore, 1997). Increases in temperature may accelerate the decomposition of SOM, thereby generating large emissions of greenhouse gases. Soil water is a controlling factor in microbial decomposition, influencing the rate and type of greenhouse gas production by limiting oxygen availability (Mu et al., 2016b). Consequently, the interplay of temperature and soil moisture will strongly influence on SOM stability during and after permafrost degradation on the TP.

Much of the TP is a grassland ecosystem, which has a large labile (easily decomposable) fraction of SOC, accounting for approximately 50% of the total SOC in the upper 10 cm soil layers (Shang et al., 2016). In these grassland ecosystems, the total water soluble organic matter contents account for approximately 15% of the total organic matter (Wu et al., 2014b). The decomposability of SOM influences how much carbon stored in soil reservoirs can be mineralized to the atmosphere after thawing. In an 80-day aerobic incubation (Chen et al., 2016), employing a carbon decomposition model on the cumulative CO_2 evolution, the authors estimated that 29.0% and 64.9% of the carbon released as CO_2 was from the fast and slow carbon pools in TP permafrost, whereas only 6.1% of CO_2 release originated from the passive C pool. In a 300-day aerobic incubation experiment at 25°C, Wu et al. (2014b) reported soil SOC mineralization of ~20%. The SOM decomposition rate in the upper layer (0–10 cm) was significantly greater than that in the lower layer (20–30 cm) (Li et al., 2018a), and the CO_2 release in permafrost layers was similar or higher than in the active layer, demonstrating the high vulnerability of carbon in permafrost-affected soils of the TP (Chen et al., 2016). Based on structural equation models, it was demonstrated that the proportion of labile carbon was one of the determinants of CO_2 release from the active layer in the TP permafrost, and soil microbial abundance was more important in carbon emissions from permafrost layers after thaw (Chen et al., 2016).

The temperature sensitivity coefficient (Q_{10}) of soil respiration is widely used to study potential greenhouse gas emissions from the decomposition of SOM. The values of Q_{10} describe the proportional change in rates of gas emission with a 10°C increase in temperature. Substrate properties and environmental variables play important roles in the variation of temperature sensitivity of CO_2 release (Ding et al., 2016b; Schädel et al., 2016; Treat et al., 2015). Based on the incubation experiments, the average temperature sensitivity coefficient (Q_{10}) values of SOM decomposition was 9.2 ± 7.1 for different depths and vegetation types (Ding et al., 2016a; Li et al., 2018a; Mu et al., 2016b) (Table 2), which is comparable with Q_{10} estimates in the circumarctic (Dutta et al., 2006; Mikan et al., 2002; Moni et al., 2015; Waldrop et al., 2010; Wickland and Neff, 2008). For deep soil layers, the sensitivities of SOM decomposition to temperature near the permafrost table and in some permafrost layers were even larger than those in surface soil layers on the TP (Mu et al., 2016b). In many models, the Q_{10} value is set at or near 2.0 (Kätterer et al., 1998; Meyer et al., 2018), though the research cited here shows that this number is not appropriate for permafrost carbon release on the TP or in the circumarctic, especially for the deep permafrost layers. Because the measured Q_{10} values for the SOM decomposition in many other soils range from 1.56 to 2.70 (Chen et al., 2010b), the high Q_{10} values in the TP permafrost regions indicate that the organic matter stored in their soils is much more vulnerable to a warming climate than soils of non-permafrost regions.

4.2. Net ecosystem carbon balance of the Tibetan Plateau

Net ecosystem carbon balance includes all the inputs and outputs of carbon, including vertical exchanges (e.g., CO_2 and CH_4 emission or uptake) and lateral fluxes (e.g., DOC and POC flux) (Chapin III et al., 2006). Empirical and modeling studies indicate that the circumarctic has been a net sink for atmospheric CO_2 of approximately 110 Tg C yr^{-1} (+291 to -80 Tg C yr^{-1}) during the growing season (Hayes et al., 2011; Mcguire et al., 2012; Schädel et al., 2016). It has recently been estimated that approximately 1,660 Tg C per winter has been released to the air from 2003-2017 based on regional in-situ observations of CO_2 from Arctic and Boreal soils (Natali et al., 2019). This is greater than the average growing season carbon uptake (~1,030 Tg per year) estimated from process models, confirming suspected decreases in the net carbon uptake of the circumarctic over the past decades (Hayes et al., 2011).

On the TP, it was found that the upper active layer currently represents a substantial regional carbon sink based on repeated soil carbon measurements in the early 2000s and 2010s at the same sites (Ding et al., 2017). However, carbon changes associated with deeper and older permafrost remain largely unknown. Many factors affect ecosystem carbon exchange, such as soil temperature and moisture, land cover types, and nitrogen deposition (Tian et al., 2017; Tian et al., 2019), yet understanding how these factors affect carbon budgets under field conditions is still lacking. As a result, there are heated debates about whether the permafrost region of the TP will be a carbon sink or source in the future (Ding et al., 2017; Yi et al., 2019; Zhao et al., 2018).

Warming can have multiple effects on ecosystem respiration and primary productivity, two of the major vertical carbon fluxes (Chapin III et al., 2006). Higher temperature can extend the growing season, potentially enhancing gross primary productivity (GPP) of vegetation (Abbott et al., 2016), but it also increases autotrophic respiration required for maintenance and growth (Abbott et al., 2016; Drake et al., 2011; Goulden et al., 2011; Kwon et al., 2019). Additionally, increasing temperature also favors the activity of heterotrophic microorganisms in the soil, further increasing carbon emission from aerobic and anaerobic respiration (Schädel et al., 2016). Plot-level warming experiments suggest that ecosystem carbon emissions of the TP will increase with warming, though the emission response rates differ between dry and wet soil conditions. In the first year that open-top chambers (OTCs) were installed in an alpine meadow, experimental warming (0.62°C increase in soil temperature) increased ecosystem respiration by 17% from June to September (Qin et al., 2015). After two years of running the OTC warming experiments, the ecosystem respiration increased by 35% in wet meadow and meadow (Mu et al., 2017a). However, warming triggered no significant increase in ecosystem respiration for the alpine steppe (Fu et al., 2013; Wang et al., 2019; Zhao et al., 2017). Likewise, four years of warming with OTCs in a wet meadow resulted in no change in carbon storage, though respiration was higher and the molecular properties of the SOM were modified (Li et al., 2020). The differences between ecosystem types could be explained by the differential autotrophic and heterotrophic responses in meadow and wet meadow versus the steppe as there is more plant biomass in the meadow and wet meadow. More plant biomass could lead to higher autotrophic respiration (Mu et al., 2017a). The temperature sensitivity of SOM decomposition in the steppe soils is also lower than in meadow and wet meadow, because the SOM under steppe is largely composed of stable organic compounds (Wu et al., 2014b). However, the intrinsic stability of some molecular compounds in soils of the TP is not always associated with their actual reactivity (Li et al., 2020). We also note that in longer-term experiments in circumarctic permafrost environments, the long-term consequences of warming can be different and even opposite the short-term effects, depending on the plant community, nutrient state, and type of warming disturbance (Bret-Harte et al., 2004; Mack et al., 2004; Shaver et al., 2001). Longer-term (i.e. >10 years) warming and nutrient manipulations are needed on the TP to constrain the initial and eventual response of the net ecosystem carbon balance to climate change.

Presently, the vertical carbon uptake of the TP will likely increase with warming, mainly in promoting plant growth and prolonging phenological periods (Xu and Xue, 2013), changing species diversity and structure (Lin et al., 2011), and increasing the net primary production (Mu et al., 2017a). Even though the carbon assimilated by plants in growing seasons is higher than the carbon emitted in the non-growing seasons, the seasonal changes in ecosystem respiration should receive more attention. In the circumarctic regions, it has been suggested that added plant growth in summer offsets little or none of the permafrost carbon released from the ecosystem via vertical and lateral fluxes year round (Abbott et al., 2016; Natali et al., 2019), and current Earth system models do not agree in magnitude or sign (McGuire et al., 2018). There are indications that additional rhizodeposition with climate warming will accelerate decomposition of previously stable SOC (Keuper et al., 2020). In the TP permafrost regions, ecosystem respiration is more sensitive to warming during the non-growing season than during the growing season. This finding indicates that winter warming could have a major effect on net ecosystem carbon balance, shifting the wet meadow and meadow ecosystem types from carbon sink to source in the near future (Mu et al., 2017a).

In addition to climate warming, hydrological changes and N deposition can also affect net ecosystem carbon balance in the TP permafrost regions. Most reports found that the alpine meadow and wet meadow ecosystems absorb more CO_2 than alpine steppe under warming conditions (Zhang et al., 2017b). The land cover types of wet meadow, meadow, and steppe are largely determined by the soil hydrological regimes, which can be changed by permafrost degradation (Cheng et al., 2019). Thaw-induced wetland drying could enhance soil CO_2 emissions on the TP (Yu et al., 2020). For alpine meadow, lowering soil moisture stimulates warming effects on net ecosystem production under wet conditions, but aggravates the drought effect under dry conditions (Quan et al., 2019). During the past decades, the N deposition rate has also been increasing along with climate warming, though there is evidence that N availability for plants has decreased due to vertical losses and changes in plant demand (Kou et al., 2018). N deposition and other changes in nutrient availability could strongly affect many ecological processes, such as soil microbial activities and the composition of the soil microbial and plant communities, resulting in changes in carbon cycling (Kou et al., 2018; Mack et al., 2004; Zong et al., 2017). In an alpine meadow, nitrogen addition increased the above-ground biomass by 14%-30% but did not significantly affect the below-ground biomass. The nitrogen addition significantly enhanced the average ecosystem respiration by approximately 50% (Bai et al., 2019). Overall, these findings suggested that the local consequences of climate change may be highly dependent on the combined effects of soil hydrology and nutrient dynamics. This represents a substantial challenge to our goal of better integrating the TP into global Earth system models, but also represents an opportunity for testing current model predictions mainly parameterized by Arctic and Boreal permafrost regions.

The CH_4 budget of the TP also shows varying roles as sink or source under different land-cover types. Alpine wetlands are expected to be an important natural source of CH_4 to the atmosphere because of their largely anoxic conditions (Chen et al., 2008). Based on eddy covariance observations, the total annual CH_4 emissions from the alpine wetland on the TP were 26.4–33.8 g CH_4 m^{-2} yr^{-1}, and the non-growing season CH_4 emissions accounted for 43.2–46.1% of the annual emissions (Song et al., 2015). However, the alpine steppe in the central TP (the Beiluhe area) is a CH_4 sink of -0.86 ± 0.23 g CH_4-C m^{-2} yr^{-1} from 2012–2016 (Yun et al., 2018), which is larger than some Arctic tundra systems due to the dryer and warmer soil conditions (Whalen, 2005; Zhuang et al., 2004). For the whole TP, the terrestrial ecosystem model (TEM) simulations suggested that the TP acts as a net CH_4 source with emissions of 0.76 Tg CH_4 y^{-1} from 1979–2000 based on a process-based ecosystem model (Jin et al., 2015). These estimates are quite different from estimates upscaled from laboratory incubations (Zhang et al., 2019c). These upscaled estimates suggest production of 0.6 Tg CH_4 y^{-1} from wet meadows and oxidation (uptake) of 10.9 Tg CH_4 y^{-1} from alpine meadows and alpine steppe (Zhang et al., 2019c). Although several sites were selected to measure CH_4 fluxes on the northern TP (Chen et al., 2010a; Mu et al., 2017c), continuous data are only available from two

Fig. 12. The field photos of thermokarst lakes on the Tibetan Plateau taken on October 30, 2019 (*a, b*) and August 30, 2019 (*c, d*). Photos *a* and *b* showed the visible bubbles at the beginning of winter, photo *d* showed the lake bank erosion.

sites, one located at northern (Whalen, 2005; Zhuang et al., 2004) and one at central TP (Yun et al., 2018). Therefore, we are yet far from reaching consensus on the role of TP permafrost as a CH_4 source or sink.

Globally, lateral carbon flux through river networks is similar in magnitude to net vertical carbon fluxes (Raymond et al., 2013; Zarnetske et al., 2018). This means that constraining lateral flux of DOC and POC is crucial to determining contemporary carbon balance estimates and predicting response to warming (Tank et al., 2020; Vonk et al., 2015). DOC concentration in TP rivers is around 2 mg C L^{-1}, lower than in many regions, attributable to relatively low ecosystem biomass on an areal basis and deep ALT (Mu et al., 2017b; Qu et al., 2017). DOC flux from the TP is estimated at 0.31 Tg C y^{-1} (Qu et al., 2017), but we could find no estimates of total POC export. The DOC in TP rivers and lakes appears to be much older than circumarctic and tropical surface waters, with a mean radiocarbon age of 500 to 700 years BP in rivers and lakes (Qu et al., 2017). This could mean that old ecosystem carbon is already being released from TP soils via hydrological leaching and transport, or that pre-aged material (e.g., coal soot) is affecting radiocarbon ages, or a combination of both. DOC biodegradability is also quite high on the TP (Mu et al., 2017b; Spencer et al., 2014), again indicating that changes in temperature and precipitation could substantially alter net ecosystem carbon balance on the TP. Increased monitoring of water discharge and water chemistry in rivers draining the TP would allow better estimates of lateral carbon flux and act as a sensitive indicator of changes in terrestrial ecosystems, including primary production, changes in SOC, and thermokarst formation (Shogren et al., 2020; Tank et al., 2020).

5. Effects of thermokarst on carbon cycling

5.1. Thaw slumps

Thaw slumps not only cause slope instability and failure, they also redistribute soil carbon and nitrogen while altering soil temperature, moisture, and oxygen availability (Abbott et al., 2014; Liu et al., 2018a; Turetsky et al., 2020). In turn, slumps may accelerate SOM decomposition, ecosystem greenhouse gas emissions, and the permafrost climate feedback (Liu et al., 2018a). Observations from thaw slumps on the TP have found a significant decrease in soil moisture, changed soil chemical characteristics such as carbon content and composition, and changes in SOC associated with iron (Liu et al., 2018a; Mu et al., 2020c). For the different land-cover types, thaw slumps on the TP lead to SOC losses of 21.0% for an alpine wet meadow, 14.4% for alpine meadows, and 17.0% for alpine steppes (Mu et al., 2020a). The effects of thaw slumps on SOC loss show considerable spatial variability in the TP permafrost region. Through the measurement of characteristic patches of net ecosystem exchange in a thermo-erosion gully, It was found that the direct disturbance of plants in exposed patches and the changes in water and nutrients decreased ecosystem carbon uptake, resulting in thaw slumps becoming a significant carbon source (Mu et al., 2017c). The ecosystem respiration following thaw slumps on the northern TP was 2.7 to 9.5-fold higher than that in similar features from Arctic and Boreal regions, suggesting that warmer and drier conditions on the TP could accelerate aerobic decomposition (Mu et al., 2017c). In the circumarctic region, formation of thermokarst landscapes can release carbon and disrupt vegetation, but it can also increase the amount of available nutrients and stimulate plant growth after stabilization (Abbott et al., 2014; Pearce et al., 2015). However, vegetation restoration appears to be extremely slow on the TP, and exposed patches disturbed by thermokarst can remain bare for decades (Liu et al., 2018a). Meanwhile, upland thermokarst formation on the TP can also enhance the CH_4 and N_2O emissions (Yang et al., 2017) like for the circumarctic (Abbott and Jones, 2015; Voigt et al., 2020). Therefore, in the long run, thaw slumps are likely to increase net greenhouse gas release from the TP.

Thaw slumps can bring SOC to the surface, potentially accelerating loss from leaching, aerobic respiration, and photooxidation (Bowen et al., 2020). Consequently, A significant decrease in the labile carbon components of organic matter and microbial decomposition rates were detected in a permafrost collapse area, which may be associated with the changes in microbial communities or cumulative leaching during

Table 3
Greenhouse gases emission from lakes on the Tibetan Plateau (TP) and other regions.

	Sites	Number of lakes	DOC (mg/L)	DIC (mg/L)	C diffusive flux (mmol m^{-2} day^{-1})	References
CH_4	Lakes in the TP permafrost	N = 3	2.4 ~ 8.2	40 ~ 817	0.03 ~ 0.4	(Yan et al., 2018)
	Thermokarst lakes in Cherskii, Siberia	N = 3	13.8 ~ 29.9	_	0.5 ~ 3.6	(Anthony et al., 2010)
	Thermokarst lakes in Yakutsk, Siberia	N = 3	_	_	2.4 ~ 8.7	(Desyatkin et al., 2009)
	Thermokarst lakes on Bylot Island, Canada	N = 21	1.5 ~ 20.8	_	0.01 ~ 5.6	(Laurion et al., 2010)
	Thermokarst lakes in Yukon-Kuskokwim Delta, Alaska	N = 4	_	_	0.1 ~ 4.8	(Bartlett et al., 1992)
	Global lakes and ponds	N = 427	_	_	0.5	(Holgerson and Raymond, 2016)
CO_2	Lakes in the TP permafrost	N = 3	2.4 ~ 8.2	40 ~ 817	30.0	(Yan et al., 2018)
	Lakes across arctic Alaska	N = 25	_	_	20.9	(Kling et al., 1991)
	Lakes in a subarctic catchment, northern Sweden	N = 27	7.0 ~ 22.0	2.5 ~ 18.4	15.0	(Lundin et al., 2013)
	Global lakes and ponds	N = 427	_	_	22.4	(Holgerson and Raymond, 2016)
	Global saline lakes	N = 196	_	714	81.0	(Duarte et al., 2008)

thermokarst formation (Wu et al., 2018a). Thaw slumps can expose organic carbon to ultraviolet radiation, which can increase DOC biodegradability during thermo-erosion (Liu et al., 2018b). Solar radiation can also directly break down SOM (Bowen et al., 2020; Olefeldt et al., 2013), though this only affects the immediate surface due to shading from soil aggregates.

To understand the net effects of thaw slumps on carbon cycling, it is necessary to clarify the processes of carbon loss, i.e., 1) How much carbon is released into the atmosphere due to microbial decomposition and photo-degradation; 2) How much carbon is transported laterally via colluvial and fluvial processes; and 3) How much carbon remains in the soils? To answer these questions, observations from thaw slumps in different stages of recovery in more regions are needed. Presently, ecosystem carbon exchanges in TP thaw slumps have been monitored in two meadow ecosystem regions (Mu et al., 2017c; Yang et al., 2017). As abrupt thaw can have a significant influence on the permafrost climate feedback (Turetsky et al., 2020), the effects of thaw slump on the loss, redistribution, and export of SOC should be examined in different land forms and land cover types.

5.2. *Thermokarst lakes*

Thermokarst lakes play an important role in vertical and lateral carbon flux in permafrost ecosystems (Fritz et al., 2015; Kling et al., 1991; Larouche et al., 2015; Shogren et al., 2019). Lateral carbon flux into lakes can be transformed into greenhouse gases (Huissteden and Dolman, 2012), and it has been estimated that the cumulative carbon released as CH_4 and CO_2 from thermokarst lakes ranged from 0.2 to 2.5 Pg C in the past 60 years in the circumarctic regions (Walter Anthony et al., 2016). As for the circumarctic, bubbling and bank erosion have been widely observed in thermokarst ponds and lakes of the TP (Fig. 12). In contrast with some circumarctic thermokarst lakes, the organic matter in the sediments of thermokarst lakes on the TP is highly decomposed (Mu et al., 2016a). N_2, O_2, and CO_2 (rather than CH_4), are the predominant constituents of the bubbles sealed in thermokarst lake ice on the TP (Wu et al., 2014a). In these lakes, the highest dissolved CO_2 and CH_4 concentrations were recorded in July, and the lowest values were recorded in September, which showed that temperature, and potentially ALT around the lake, affected greenhouse gas release (Mu et al., 2016a).

The average diffusive carbon flux from saline and non-saline lakes in the TP permafrost regions was 73.7 mmol m^{-2} day^{-1} for CO_2 and 5.2 mmol m^{-2} day^{-1} for CH_4 (Yang et al., 2018). This CO_2 efflux is lower than from saline lakes globally (Duarte et al., 2008), but larger than Arctic lakes in northern Alaska (Kling et al., 1991), lakes in northern Sweden (Lundin et al., 2013), and global lakes and ponds (Holgerson and Raymond, 2016) (Table 3). The high CO_2 eflux from lakes on the TP can be attributed to several mechanisms: 1) The TP thermokarst lakes have higher DOC contents than global lakes and ponds because the catchments in the permafrost regions have high SOC contents; 2) The TP water temperature is higher than those in the circumarctic regions in summer because the TP has a lower latitude; and 3) Dissolved inorganic carbon (DIC) in the TP lakes may contribute to the CO_2 flux because these saline lakes have high pH values (8.53 to 10.2), and DIC is present mostly in the form of CO_3^{2-} or HCO_3^- (Mu et al., 2016a). The CH_4 diffusive flux in the TP lakes is substantially lower than in most thermokarst lakes of the circumarctic regions such as Siberia, Canada, and Alaska (Table 3). This may be attributed to differences in the properties of permafrost-affected organic carbon and water chemistry between TP lakes and circumarctic thermokarst lakes. Many TP lakes belong to the sulfate type, in which CH_4 production can be inhibited and any added CH_4 can be oxidized by SO_4^{2-} via anaerobic oxidation (Yang et al., 2018). This is in line with observations from the Arctic, where high sulfate lakes and streams show low CH_4 concentration (Abbott et al., 2015b). So far, the greenhouse gas emission rates and biogeochemical processes in thermokarst lakes on the TP have been poorly evaluated, which hampers the predictive power of the effects of climate warming on carbon fluxes in the TP permafrost regions.

6. Modelling net ecosystem carbon balance of TP permafrost regions

Vegetation greenness has been increasing together with regional warming on the TP and surrounding areas (Piao et al., 2020). Some ecosystem and Earth-system models have been used to simulate the carbon budget on the TP. From 1961 to 2010, alpine grasslands on the TP acted as a carbon sink with a mean annual value of 10.1-11.8 Tg C yr^{-1} (Piao et al., 2012; Yan et al., 2015). The TP was found to be a net carbon sink of 30.1 Tg C year^{-1} during the 1980s-1990s (Piao et al., 2009) and 35.8 Tg C year^{-1} during the 1990s (Zhuang et al., 2010). These reports of TP carbon balance only considered the effects of climate change, without the consideration of the effects of permafrost on SOC stocks and turnover. Changes in permafrost conditions undoubtedly affect the carbon dynamics of the TP. Moreover, there are large discrepancies among estimates of regional soil respiration (Wang et al., 2002; Zhuang et al., 2010), which resulted in large uncertainty in the net carbon budget. It has been suggested that research priority should be given to investigating the major controls on and processes of SOM decomposition and carbon pool sizes (Cheng et al., 2019).

For the future projections of the carbon balance on the TP, six Earth-

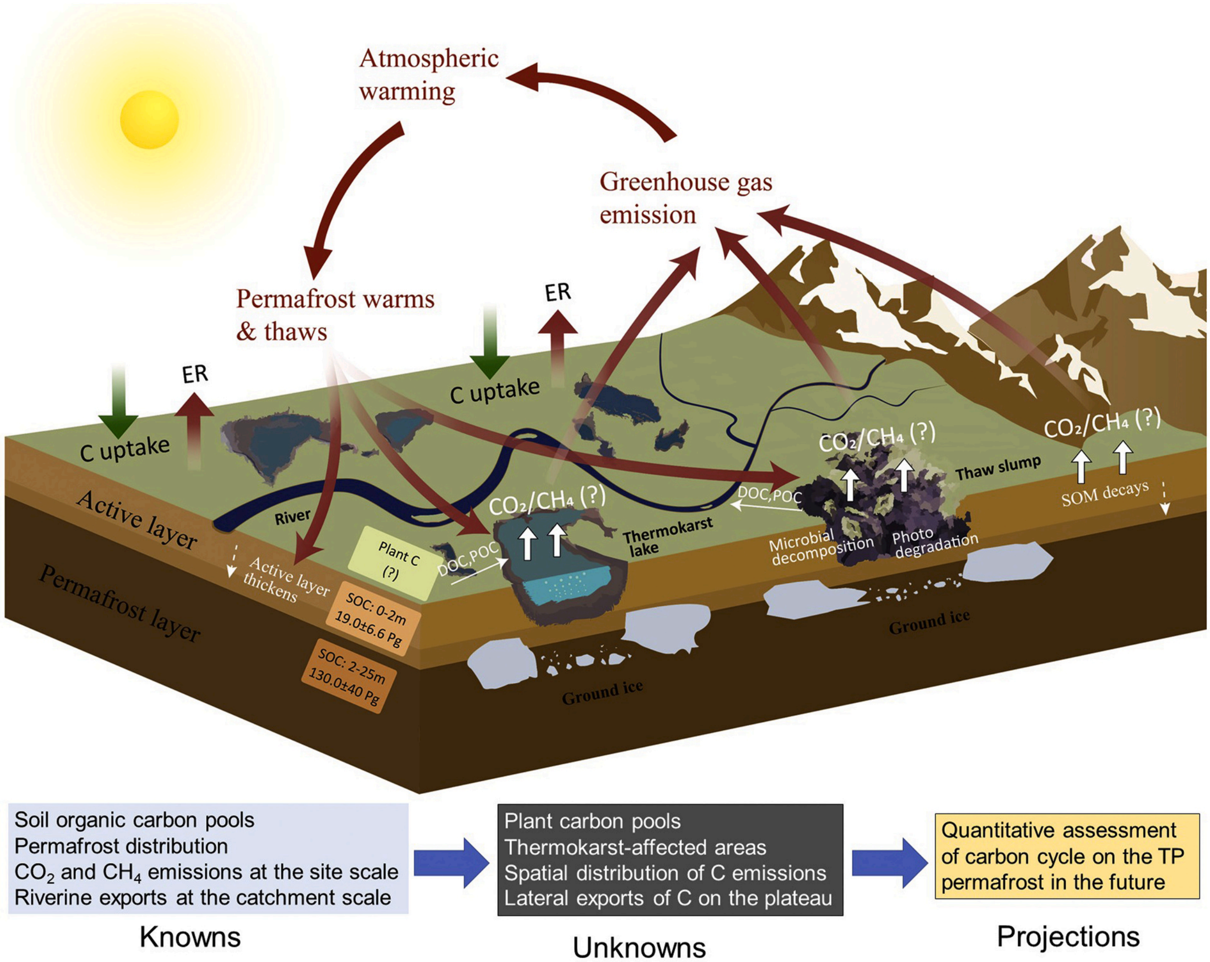

Fig. 13. Conceptual model of the permafrost carbon cycle on the Tibetan Plateau with arrows representing responses to climate change. The red arrows show feedback between warming and greenhouse gas release, including ecosystem respiration (ER). Warming leads to permafrost degradation and subsequent greenhouse gas production. The green arrows show the effects of warming on vegetation growth, which can allow greater carbon uptake during the growing seasons. The white upward errors show the CO_2 and CH_4 emissions from thermokarst lakes, thaw slumps (microbial degradation and photo-degradation of organic matter), and *in situ* decomposition of soil organic matter (SOM). The white horizontal arrows show lateral DOC and POC transport into surface water networks.

system models in phase 5 of the Coupled Model Inter-comparison Project (CMIP5) showed that the TP would uptake more carbon than presently from the atmosphere from 2006–2100 under RCP4.5 scenario (Li et al., 2015). In these models, the permafrost climate feedback is not yet included within the coupled earth system models in the CMIP5 analysis (Burke et al., 2013). Furthermore, ecosystem and Earth-system models simulate slow and steady permafrost degradation, ignoring the effects of abrupt permafrost collapse and expansion of thermokarst terrains on carbon release (Turetsky et al., 2020). Therefore, filling the gaps on the impacts of thawing permafrost on carbon balance in mountainous permafrost will improve our understanding of climate change in this region and globally.

7. Summary and prospects

Our review summarizes the current knowledge and gaps in permafrost degradation and its effect on the carbon cycle on the Third Pole. We summarize many of the central observations and hypothesis in Fig. 13. Presently, permafrost degradation is occurring widely on the TP, while the spatial distribution of permafrost observations and thermokarst monitoring networks is very uneven. SOC storage in TP permafrost regions has large uncertainties, ranging from 8.5 to 17.8 Pg for 0-1 m and 12.2 to 27.9 Pg for 0-2 m. The temperature sensitivity coefficient (Q_{10}) of SOC decomposition has been estimated to range from 2.1 to 20.8, similar to circumarctic regions. From the available field manipulations (usually <10 years of OTC warming), it appears that warming can increase carbon assimilation in alpine wet meadows and alpine meadows during the growing season, while there is no significant effect for the alpine steppe. Thaw slumps can accelerate SOC loss, and the thermokarst lakes have higher CO_2 but lower CH_4 emissions in comparison with the circumarctic regions, because of the differences in SOM characteristics, microbial decomposition, photo-degradation, and vegetation restoration rates (Fig. 13). However, observations from thaw slumps are limited to one ecosystem type (alpine meadow), substantially limiting our ability to upscale thermokarst effects to the entire TP.

The key issues we encountered that need further research can be divided into the following three aspects. (1) Insufficient data of SOC content and composition. This is especially true for the central and western TP, where large areas have no quantitative SOC data for different soil layers. While there are multiple extrapolation methods to calculate the SOC pools for the TP permafrost regions, until the distribution of soil depths and observations of SOC stocks are available, substantial uncertainty will remain. (2) The relationships among SOC, soil water, and temperature need to be established. While it is not logistically feasible to monitor carbon cycle processes, including vegetation growth, soil respiration, and soil water and temperature at hundreds of sites simultaneously, strategic maintenance of long-term ecological stations at multiple stations across ecosystem types and regions on the TP should be a priority. Using representative continuous monitoring data, it will be possible to improve the land surface models and dynamic vegetation models to simulate the carbon cycle in the future. (3) Thermokarst terrains, including thaw slump and thermokarst lakes, should be considered in the future permafrost carbon cycle on the TP. Understanding the area of thermokarst terrains and the carbon release rates from these terrains would be useful to assess the regional carbon cycle on the TP.

Author contributions

C.C. Mu, B. Abbott, M. Mu, C.Y. Fan, X. Chen, L. Jia, T. Zhang, and X. D. Wu wrote the first draft of the manuscript. R.M. Yang, K. Wang and X. Q. Peng provided the research data for the article. C.C. Mu, B. Abbott, A. Norris, Q.B. Wu, G. Guggenberger, and X.D. Wu, reviewed and edited the manuscript before submission. B.W. Abbott and A.J. Norris performed the meta-analysis of citations and revised the manuscript. All authors made substantial contributions to the discussion of content.

Declaration of Competing Interest

The authors declare that they have no known competing financial interests or personal relationships that could have appeared to influence the work reported in this paper.

Acknowledgements

This work was supported by the second Tibetan Plateau Scientific Expedition and Research Program (STEP) (2019QZKK0605), the foundation of State Key Laboratory of Cryospheric Science (SKLCS-ZZ-2020), the National Natural Science Foundation of China (41721091, 41941015, 41871050), the National Key Research and Development Program of China (2019YFA0607003, 2019YFC1509104), and the Open Foundations of the State Key Laboratory of Frozen Soil Engineering (Grant No. SKLFSE201705). B.W. Abbott and A.J. Norris were supported by the U.S. National Science Foundation award number 1916565, and G. Guggenberger acknowledges support by the German Research Foundation (DFG) (GRK 2309/1).

References

Abbott, B.W., Larouche, J.R., Jones, J.B., Bowden, W.B., Balser, A.W., 2014. Elevated dissolved organic carbon biodegradability from thawing and collapsing permafrost. J. Geophys. Res. Biogeosci. 119 (10), 2049–2063.

Abbott, B.W., Jones, J.B., Godsey, S.E., Larouche, J.R., Bowden, W.B., 2015b. Patterns and persistence of hydrologic carbon and nutrient export from collapsing upland permafrost. Biogeosciences 12 (12), 3725–3740.

Abbott, Benjamin W, Jones, Jeremy B, 2015. Permafrost collapse alters soil carbon stocks, respiration, CH_4, and N_2O in upland tundra. Global Change Biology 21 (12), 4570–4587.

Abbott, B.W., Jones, J.B., Edward, A.G.S., Chapin III, F.S., Bowden, W.B., Bret-Harte, M. S., Epstein, H.E., Flannigan, M.D., Harms, T.K., Hollingsworth, T.N., Mack, M.C., McGuire, A.D., Natali, S.M., Rocha, A.V., Tank, S.E., Turetsky, M.R., Vonk, J.E., Wickland, K.P., Aiken, G.R., Alexander, H.D., Amon, R.M.W., Benscoter, B.W., Bergeron, Y., Bishop, K., Blarquez, O., Bond-Lamberty, B., Breen, A.L., Buffam, I., Cai, Y., Carcaillet, C., Carey, S.K., Chen, J.M., Chen, H.Y.H., Christensen, T.R., Cooper, L.W., Cornelissen, J.H.C., Groot, W.J.D., DeLuca, T.H., Dorrepaal, E., Fetcher, N., Finlay, J.C., Forbes, B.C., French, N.H.F., Gauthier, S., Girardin, M.P., Goetz, S.J., Goldammer, J.G., Gough, L., Grogan, P., Guo, L., Higuera, P.E., Hinzman, L., Hu, F.S., Hugelius, G., Jafarov, E.E., Jandt, R., Johnstone, J.F., Karlsson, J., Kasischke, E.S., Kattner, G., Kelly, R., Keuper, F., Kling, G.W., Kortelainen, P., Kouki, J., Kuhry, P., Laudon, H., Laurion, I., Macdonald, R.W., Mann, P.J., Martikainen, P.J., McClelland, J.W., Molau, U., Oberbauer, S.F., Olefeldt, D., Paré, D., Parisien, M.-A., Payette, S., Peng, C., Pokrovsky, O.S., Rastetter, E.B., Raymond, P.A., Raynolds, M.K., Rein, G., Reynolds, J.F., Robards, M., Rogers, B.M., Schädel, C., Schaefer, K., Schmidt, I.K., Shvidenko, A., Sky, J., Spencer, R.G.M., Starr, G., Striegl, R.G., Teisserenc, R., Tranvik, L.J., Virtanen, T., Welker, J.M., Zimov, S., 2016. Biomass offsets little or none of permafrost carbon release from soils, streams, and wildfire: an expert assessment. Environ. Res. Lett. 11 (3), 034014.

Abbott, B.W., Gruau, G., Zarnetske, J.P., Moatar, F., Barbe, L., Thomas, Z., Fovet, O., Kolbe, T., Gu, S., Pierson-Wickmann, A.C., Davy, P., Pinay, G., 2018. Unexpected spatial stability of water chemistry in headwater stream networks. Ecol. Lett. 21 (2), 296–308.

AMAP, 2017. Snow, Water, Ice and Permafrost in the Arctic (SWIPA) 2017. In: Arctic Monitoring and Assessment Programme (AMAP), Oslo, Norway. xiv +, p. 269.

AMAP, 2019. AMAP Strategic Framework 2019+, Norway, pp. 1–8.

Anthony, K.M.W., Vas, D., Brosius, L., Chapin, F.S., Zimov, S., Zhuang, Q., 2010. Estimating methane emissions from northern lakes using ice-bubble surveys. Limnol. Oceanogr. Methods 8 (11), 592–609.

Anthony, W.K.M., Zimov, S.A., Grosse, G., Jones, M.C., Anthony, P.M., Chapin III, F.S., Finlay, J.C., Mack, M.C., Davydov, S.P., Frenzel, P., 2014. A shift of thermokarst lakes from carbon sources to sinks during the Holocene epoch. Nature 511, 452–456.

Bai, W., Xi, J.Y., Wang, G.X., 2019. Effects of short-term warming and nitrogen addition on CO_2 emission during growing season in an alpine swamp meadow ecosystem of Qinghai-Tibetan Plateau. Chin. J. Ecol. 38 (4), 927–936.

Balser, A.W., Jones, J.B., Gens, R., 2014. Timing of retrogressive thaw slump initiation in the Noatak Basin, northwest Alaska, USA. J. Geophys. Res. Earth Surf. 119 (5), 1106–1120.

Bartlett, K.B., Crill, P.M., Sass, R.L., Harriss, R.C., Dise, N.B., 1992. Methane emissions from tundra environments in the Yukon-Kuskokwim delta, Alaska. J. Geophys. Res.-Atmos. 97 (D15), 16645–16660.

Baumann, F., He, J.-S., Schmidt, K., Kühn, P., Scholten, T., 2009a. Pedogenesis, permafrost, and soil moisture as controlling factors for soil nitrogen and carbon contents across the Tibetan Plateau. Glob. Chang. Biol. 15 (12), 3001–3017.

Baumann, F., He, J., Schmidt, K., Kühn, P., Scholten, T., 2009b. Pedogenesis, permafrost, and soil moisture as controlling factors for soil nitrogen and carbon contents across the Tibetan Plateau. Glob. Chang. Biol. 15 (12), 3001–3017.

Biskaborn, B.K., Smith, S.L., Noetzli, J., Matthes, H., Vieira, G., Streletskiy, D.A., Schoeneich, P., Romanovsky, V.E., Lewkowicz, A.G., Abramov, A., Allard, M., Boike, J., Cable, W.L., Christiansen, H.H., Delaloye, R., Diekmann, B., Drozdov, D., Etzelmüller, B., Grosse, G., Guglielmin, M., Ingeman-Nielsen, T., Isaksen, K., Ishikawa, M., Johansson, M., Johannsson, H., Joo, A., Kaverin, D., Kholodov, A., Konstantinov, P., Kröger, T., Lambiel, C., Lanckman, J.-P., Luo, D., Malkova, G., Meiklejohn, I., Moskalenko, N., Oliva, M., Phillips, M., Ramos, M., Sannel, A.B.K., Sergeev, D., Seybold, C., Skryabin, P., Vasiliev, A., Wu, Q., Yoshikawa, K., Zheleznyak, M., Lantuit, H., 2019. Permafrost is warming at a global scale. Nat. Commun. 10 (1), 264.

Bockheim, J., 2007. Importance of cryoturbation in redistributing organic carbon in permafrost-affected soils. Soil Sci. Soc. Am. J. 71 (4), 1335–1342.

Bockheim, J.G., Munroe, J.S., 2014. Organic carbon pools and genesis of alpine soils with permafrost: A review. Arct. Antarct. Alp. Res. 46 (4), 987–1006.

Bowden, W.B., Gooseff, M.N., Balser, A., Green, A., Peterson, B.J., Bradford, J., 2008. Sediment and nutrient delivery from thermokarst features in the foothills of the North Slope, Alaska: Potential impacts on headwater stream ecosystems. J. Geophys. Res. Biogeosci. 113 (G2), G02026.

Bowen, J.C., Ward, C.P., Kling, G.W., Cory, R.M., 2020. Arctic amplification of global warming strengthened by sunlight oxidation of permafrost carbon to CO_2. Geophys. Res. Lett. 47 (12) e2020GL087085.

Bret-Harte, M.S., Garca, E.A., SacrÉ, V.M., Whorley, J.R., Wagner, J.L., Lippert, S.C., Chapin III, F.S., 2004. Plant and soil responses to neighbour removal and fertilization in Alaskan tussock tundra. J. Ecol. 92 (4), 635–647.

Brown, I.E., Ferrians, O.J., Heginbottom, J.A., Melnikov, E.S., Regional, J.Å., 2002. Circum-Arctic map of permafrost and ground-ice conditions Version 2, Center for Integrated Data Analytics Wisconsin Science Center. National Snow and Ice Data Center, Boulder, Colorado USA, NSIDC.

Burke, E.J., Jones, C.D., Koven, C.D., 2013. Estimating the Permafrost-Carbon Climate Response in the CMIP5 Climate Models Using a Simplified Approach. J. Clim. 26 (14), 4897–4909.

Burn, C.R., 1998. The response (1958-1997) of permafrost and near-surface ground temperatures to forest fire, Takhini River valley, southern Yukon Territory. Can. J. Earth Sci. 35 (2), 184–199.

Cao, B., Zhang, T., Peng, X., Mu, C., Wang, Q., Zheng, L., Wang, K., Zhong, X., 2018. Thermal characteristics and recent changes of permafrost in the Upper Reaches of the Heihe River Basin, Western China. J. Geophys. Res.-Atmos. 123 (15), 7935–7949.

Cao, B., Zhang, T., Wu, Q., Sheng, Y., Zhao, L., Zou, D., 2019. Permafrost zonation index map and statistics over the Qinghai–Tibet Plateau based on field evidence. Permafr. Periglac. Process. 30 (3), 178–194.

Carey, J.C., Abbott, B.W., Rocha, A.V., 2019. Plant uptake offsets silica release from a large Arctic tundra wildfire. Earth's Future 7 (9), 1044–1057.

Chapin III, F.S., Woodwell, G.M., Randerson, J.T., Rastetter, E.B., Lovett, G.M., Baldocchi, D.D., Clark, D.A., Harmon, M.E., Schimel, D.S., Valentini, R., Wirth, C., Aber, J.D., Cole, J.J., Goulden, M.L., Harden, J.W., Heimann, M., Howarth, R.W., Matson, P.A., McGuire, A.D., Melillo, J.M., Mooney, H.A., Neff, J.C., Houghton, R.A., Pace, M.L., Ryan, M.G., Running, S.W., Sala, O.E., Schlesinger, W.H., Schulze, E.D., 2006. Reconciling Carbon-cycle Concepts, Terminology, and Methods. Ecosystems 9 (7), 1041–1050.

Chen, H., Yao, S., Wu, N., Wang, Y., Luo, P., Tian, J., Gao, Y., Sun, G., 2008. Determinants influencing seasonal variations of methane emissions from alpine wetlands in Zoige Plateau and their implications. J. Geophys. Res.-Atmos. 113 (D12), D12303.

Chen, H., Wu, N., Yao, S., Gao, Y., Wang, Y., Tian, J., Yuan, X., 2010a. Diurnal variation of methane emissions from an alpine wetland on the eastern edge of Qinghai-Tibetan Plateau. Environ. Monit. Assess. 164 (1), 21–28.

Chen, X., Tang, J., Jiang, L., Li, B., Chen, J., Fang, C., 2010b. Evaluating the impacts of incubation procedures on estimated Q_{10} values of soil respiration. Soil Biol. Biochem. 42 (12), 2282–2288.

Chen, H., Zhu, Q., Peng, C., Wu, N., Wang, Y., Fang, X., Gao, Y., Zhu, D., Yang, G., Tian, J., Kang, X., Piao, S., Ouyang, H., Xiang, W., Luo, Z., Jiang, H., Song, X., Zhang, Y., Yu, G., Zhao, X., Gong, P., Yao, T., Wu, J., 2013. The impacts of climate change and human activities on biogeochemical cycles on the Qinghai-Tibetan Plateau. Glob. Chang. Biol. 19 (10), 2940–2955.
Chen, L., Liang, J., Qin, S., Liu, L., Fang, K., Xu, Y., Ding, J., Li, F., Luo, Y., Yang, Y., 2016. Determinants of carbon release from the active layer and permafrost deposits on the Tibetan Plateau. Nat. Commun. 7, 13046.
Cheng, G., Zhao, L., Li, R., Wu, X., Sheng, Y., Hu, G., Zou, D., Jin, H., Li, X., Wu, Q., 2019. Characteristic, changes and impacts of permafrost on Qinghai-Tibet Plateau. Chin. Sci. Bull. 64, 2783–2795.
Coolen, M.J., van de Giessen, J., Zhu, E.Y., Wuchter, C., 2011. Bioavailability of soil organic matter and microbial community dynamics upon permafrost thaw. Environ. Microbiol. 13 (8), 2299–2314.
Desyatkin, A.R., Takakai, F., Fedorov, P.P., Nikolaeva, M.C., Hatano, R., 2009. CH4 emission from different stages of thermokarst formation in Central Yakutia, East Siberia. Soil Sci. Plant Nutr. 55 (4), 558–570.
Ding, J., Chen, L., Zhang, B., Liu, L., Yang, G., Fang, K., Chen, Y., Li, F., Kou, D., Ji, C., Luo, Y., Yang, Y., 2016a. Linking temperature sensitivity of soil CO2 release to substrate, environmental, and microbial properties across alpine ecosystems. Glob. Biogeochem. Cycles 30 (9), 1310–1323.
Ding, J., Li, F., Yang, G., Chen, L., Zhang, B., Liu, L., Fang, K., Qin, S., Chen, Y., Peng, Y., Ji, C., He, H., Smith, P., Yang, Y., 2016b. The permafrost carbon inventory on the Tibetan Plateau: a new evaluation using deep sediment cores. Glob. Chang. Biol. 22 (8), 2688–2701.
Ding, J., Chen, L., Ji, C., Hugelius, G., Li, Y., Liu, L., Qin, S., Zhang, B., Yang, G., Li, F., Fang, K., Chen, Y., Peng, Y., Zhao, X., He, H., Smith, P., Fang, J., Yang, Y., 2017. Decadal soil carbon accumulation across Tibetan permafrost regions. Nat. Geosci. 10 (6), 420–424.
Ding, J., Wang, T., Piao, S., Smith, P., Zhang, G., Yan, Z., Ren, S., Liu, D., Wang, S., Chen, S., 2019a. The paleoclimatic footprint in the soil carbon stock of the Tibetan permafrost region. Nat. Commun. 10, 4195.
Ding, Y., Zhang, S., Zhao, L., Li, Z., Kang, S., 2019b. Global warming weakening the inherent stability of glaciers and permafrost. Sci. Bull. 64 (4), 245–253.
Dorfer, C., Kühn, P., Baumann, F., He, J.S., Scholten, T., 2013. Soil organic carbon pools and stocks in permafrost-affected soils on the Tibetan plateau. PLoS One 8 (2), e57024.
Drake, J.E., Davis, S.C., Raetz, L.M., Delucia, E.H., 2011. Mechanisms of age-related changes in forest production: the influence of physiological and successional changes. Glob. Chang. Biol. 17 (4), 1522–1535.
Du, C., Gao, Y., 2020. Opposite patterns of soil organic and inorganic carbon along a climate gradient in the alpine steppe of northern Tibetan Plateau. Catena 186, 104366.
Duarte, C.M., Prairie, Y.T., Montes, C., Cole, J.J., Striegl, R., Melack, J., Downing, J.A., 2008. CO2 emissions from saline lakes: A global estimate of a surprisingly large flux. J. Geophys. Res. Biogeosci. 113, G04041.
Dutta, K., Schuur, E.A.G., Neff, J.C., Zimov, S.A., 2006. Potential carbon release from permafrost soils of Northeastern Siberia. Glob. Chang. Biol. 12 (12), 2336–2351.
Egelkraut, D., Aronsson, K.-Å., Allard, A., Åkerholm, M., Stark, S., Olofsson, J., 2018. Multiple feedbacks contribute to a centennial legacy of reindeer on tundra vegetation. Ecosystems 21 (8), 1545–1563.
Elberling, B., Michelsen, A., Schädel, C., Schuur, E.A., Christiansen, H.H., Berg, L., Tamstorf, M.P., Sigsgaard, C., 2013. Long-term CO_2 production following permafrost thaw. Nat. Clim. Chang. 3 (10), 890–894.
Fang, J., Liu, G., Xu, S., 1996. Soil carbon pool in China and its global significance. J. Environ. Sci. 2, 249–254.
Farquharson, L.M., Romanovsky, V.E., Cable, W.L., Walker, D.A., Kokelj, S.V., Nicolsky, D., 2019. Climate change drives widespread and rapid thermokarst development in very cold permafrost in the Canadian High Arctic. Geophys. Res. Lett. 46 (12), 6681–6689.
Fritz, M., Opel, T., Tanski, G., Herzschuh, U., Meyer, H., Eulenburg, A., Lantuit, H., 2015. Dissolved organic carbon (DOC) in Arctic ground ice. Cryosphere 9 (1), 77–114.
Fu, Y.H., Campioli, M., Deckmyn, G., Janssens, I.A., 2013. Sensitivity of leaf unfolding to experimental warming in three temperate tree species. Agric. For. Meteorol. 181 (21), 125–132.
Gao, T., Kang, S., Chen, R., Zhang, T., Zhang, T., Han, C., Tripathee, L., Sillanpää, M., Zhang, Y., 2019. Riverine dissolved organic carbon and its optical properties in a permafrost region of the Upper Heihe River basin in the Northern Tibetan Plateau. Sci. Total Environ. 686, 370–381.
Gentsch, N., Mikutta, R., Alves, R.J.E., Barta, J., Capek, P., Gittel, A., Hugelius, G., Kuhry, P., Lashchinskiy, N., Palmtag, J., Richter, A., Šantrůčková, H., Schnecker, J., Shibistova, O., Urich, T., Wild, B., Guggenberger, G., 2015. Storage and transformation of organic matter fractions in cryoturbated permafrost soils across the Siberian Arctic. Biogeosciences 12 (14), 4525–4542.
Gentsch, N., Wild, B., Mikutta, R., Čapek, P., Diáková, K., Schrumpf, M., Turner, S., Minnich, C., Schaarschmidt, F., Shibistova, O., Schnecker, J., Urich, T., Gittel, A, Šantrůčková, H., Bárta, J., Lashchinskiy, N., Fuß, R., Richter, A., Guggenberger, G., 2018. Temperature response of permafrost soil carbon is attenuated by mineral protection. Glob. Chang. Biol. 24 (8), 3401–3415.
Giardina, C.P., Ryan, M.G., 2000. Evidence that decomposition rates of organic carbon in mineral soil do not vary with temperature. Nature 404 (6780), 858–861.
Goulden, M.L., Mcmillan, A.M.S., Winston, G.C., Rocha, A.V., Manies, K.L., Harden, J.W., Bond-Lamberty, B.P., 2011. Patterns of NPP, GPP, respiration, and NEP during boreal forest succession. Glob. Chang. Biol. 17 (2), 855–871.
Grosse, G., Romanovsky, V., Walter, K., Morgenstern, A., Zimov, S., 2008. Distribution of Thermokarst Lakes and Ponds at Three Yedoma Sites in Siberia, pp. 551–556.
Guo, D., Wang, H., Li, D., 2012. A projection of permafrost degradation on the Tibetan Plateau during the 21st century. J. Geophys. Res.-Atmos. 117 (D5), D05106.
Hayes, D.J., McGuire, A.D., Kicklighter, D.W., Gurney, K.R., Burnside, T.J., Melillo, J.M., 2011. Is the northern high-latitude land-based CO2 sink weakening? Glob. Biogeochem. Cycles 25 (3), GB3018.
Hinkel, K.M., Jones, B.M., Eisner, W.R., Cuomo, C.J., Beck, R.A., Frohn, R., 2007. Methods to assess natural and anthropogenic thaw lake drainage on the western Arctic coastal plain of northern Alaska. J. Geophys. Res. Earth Surf. 112. F02S16.
Hinkel, K.M., Sheng, Y., Lenters, J.D., Lyons, E.A., Beck, R.A., Eisner, W.R., Wang, J., 2012. Thermokarst Lakes on the Arctic Coastal Plain of Alaska: Geomorphic Controls on Bathymetry. Permafr. Periglac. Process. 23 (3), 218–230.
Hobbie, S.E., Schimel, J.P., Trumbore, S.E., Randerson, J.R., 2000. Controls over carbon storage in high-latitude soils. Glob. Chang. Biol. 6 (S1), 196–210.
Hock, R., Rasul, G., Adler, C., Cáceres, B., Gruber, S., Hirabayashi, Y., Jackson, M., Kääb, A., Kang, S., Kutuzov, S., Milner, A., Molau, U., Morin, S., Orlove, B., Steltzer, H., Allen, S., Arenson, L., Baneerjee, S., Barr, I., Bórquez, R., Brown, L., Cao, B., Carey, M., Cogley, G., Fischlin, A., de Sherbinin, A., Eckert, N., Geertsema, M., Hagenstad, M., Honsberg, M., Hood, E., Huss, M., Jimenez Zamora, E., Kotlarski, S., Lefeuvre, P.M., Ignacio López Moreno, J., Lundquist, J., McDowell, G., Mills, S., Mou, C., Nepal, S., Noetzli, J., Palazzi, E., Pepin, N., Rixen, C., Shahgedanova, M., McKenzie Skiles, S., Vincent, C., Viviroli, D., Weyhenmeyer, G.A., Yangjee Sherpa, P., Weyer, N., Wouters, B., Yasunari, T., You, Q., Zhang, Y., 2019. High Mountain Areas. In: IPCC Special Report on the Ocean and Cryosphere in a Changing Climate.
Holgerson, M.A., Raymond, P.A., 2016. Large contribution to inland water CO2 and CH4 emissions from very small ponds. Nat. Geosci. 9, 222–226.
Hopping, K.A., Knapp, A.K., Dorji, T., Klein, J.A., 2018. Warming and land use change concurrently erode ecosystem services in Tibet. Glob. Chang. Biol. 24 (11), 5534–5548.
Hu, G., Fang, H., Liu, G., Zhao, L., Wu, T., Li, R., Wu, X., 2014. Soil carbon and nitrogen in the active layers of the permafrost regions in the Three Rivers' Headstream. Environ. Earth Sci. 72 (12), 5113–5122.
Hu, G., Zhao, L., Li, R., Wu, X., Wu, T., Xie, C., Zhu, X., Su, Y., 2019. Variations in soil temperature from 1980 to 2015 in permafrost regions on the Qinghai-Tibetan Plateau based on observed and reanalysis products. Geoderma 337, 893–905.
Huang, L., Liu, L., Jiang, L., Zhang, T., 2018. Automatic Mapping of Thermokarst Landforms from Remote Sensing Images Using Deep Learning: A Case Study in the Northeastern Tibetan Plateau. Remote Sens. 10 (12), 2067.
Huang, L., Luo, J., Lin, Z., Niu, F., Liu, L., 2020. Using deep learning to map retrogressive thaw slumps in the Beiluhe region (Tibetan Plateau) from CubeSat images. Remote Sens. Environ. 237, 111534.
Hugelius, G., Strauss, J., Zubrzycki, S., Harden, J.W., Schuur, E., Ping, C.-L., Schirrmeister, L., Grosse, G., Michaelson, G.J., Koven, C.D., 2014. Estimated stocks of circumpolar permafrost carbon with quantified uncertainty ranges and identified data gaps. Biogeosciences 11 (23), 6573–6593.
Huissteden, J.V., Dolman, A., 2012. Soil carbon in the Arctic and the permafrost carbon feedback. Curr. Opin. Environ. Sustain. 4 (5), 545–551.
In't Zandt, M.H., Liebner, S., Welte, C.U., 2020. Roles of thermokarst lakes in a warming world. Trends Microbiol. 28 (9), 760–779.
Jiang, L., Chen, H., Zhu, Q., Yang, Y., Li, M., Peng, C., Zhu, D., He, Y., 2018. Assessment of frozen ground organic carbon pool on the Qinghai-Tibet Plateau. J. Soils Sediments 19 (1), 128–139.
Jin, H.J., Chang, X.L., Wang, S.L., 2007. Evolution of permafrost on the Qinghai-Xizang (Tibet) Plateau since the end of the late Pleistocene. J. Geophys. Res. Earth Surf. 112. F02S09.
Jin, Z., Zhuang, Q., He, J.S., Zhu, X., Song, W., 2015. Net exchanges of methane and carbon dioxide on the Qinghai-Tibetan Plateau from 1979 to 2100. Environ. Res. Lett. 10, 085007.
Jorgenson, M.T., Osterkamp, T.E., 2005. Response of boreal ecosystems to varying modes of permafrost degradation. Can. J. For. Res. 35 (9), 2100–2111.
Jorgenson, M.T., Shur, Y.L., Osterkamp, T.E., 2008. Thermokarst in Alaska. In: Fairbanks, Alaska, Kane, D.L., Hinkel, K.M. (Eds.), Proceedings of the Ninth International Conference on Permafrost, 29 June– 3 July 2008. Institute of Northern Engineering, University of Alaska Fairbanks, Fairbanks, Alaska, pp. 869–876.
Kang, S., Xu, Y., You, Q., Flügel, W.-A., Pepin, N., Yao, T., 2010. Review of climate and cryospheric change in the Tibetan Plateau. Environ. Res. Lett. 5 (1), 015101.
Kang, S., Zhang, Q., Qian, Y., Ji, Z., Li, C., Cong, Z., Zhang, Y., Guo, J., Du, W., Huang, J., You, Q., Panday, A.K., Rupakheti, M., Chen, D., Gustafsson, Ö., Thiemens, M.H., Qin, D., 2019. Linking atmospheric pollution to cryospheric change in the Third Pole region: current progress and future prospects. Natl. Sci. Rev. 6 (4), 796–809.
Kätterer, T., Reichstein, M., Andrén, O., Lomander, A., 1998. Temperature dependence of organic matter decomposition: a critical review using literature data analyzed with different models. Biol. Fertil. Soils 27 (3), 258–262.
Keuper, F., Wild, B., Kummu, M., Beer, C., Blume-Werry, G., Fontaine, S., Gavazov, K., Gentsch, N., Guggenberger, G., Hugelius, G., Jalava, M., Koven, C., Krab, E.J., Kuhry, P., Monteux, S., Richter, A., Shahzad, T., Weedon, J.T., Dorrepaal, E., 2020. Carbon loss from northern circumpolar permafrost soils amplified by rhizosphere priming. Nat. Geosci. 13 (8), 560–565.
Kirdyanov, A.V., Saurer, M., Siegwolf, R., Knorre, A.A., Prokushkin, A.S., Churakova, O. V., Fonti, M.V., Büntgen, U., 2020. Long-term ecological consequences of forest fires in the continuous permafrost zone of Siberia. Environ. Res. Lett. 15 (3), 034061.
Kling, G.W., Kipphut, G.W., Miller, M.C., 1991. Arctic Lakes and Streams as Gas Conduits to the Atmosphere: Implications for Tundra Carbon Budgets. Science 251 (4991), 298–301.
Kokelj, S.V., Jorgenson, M.T., 2013. Advances in thermokarst research. Permafr. Periglac. Process. 24 (2), 108–119.

Kou, D., Peng, Y., Wang, G., Ding, J., Chen, Y., Yang, G., Fang, K., Liu, L., Zhang, B., Müller, C., Zhang, J., Yang, Y., 2018. Diverse responses of belowground internal nitrogen cycling to increasing aridity. Soil Biol. Biochem. 116, 189–192.

Kuang, X., Jiao, J.J., 2016. Review on climate change on the Tibetan Plateau during the last half century. J. Geophys. Res.-Atmos. 121 (8), 3979–4007.

Kwon, M.J., Natali, S.M., Hicks Pries, C.E., Schuur, E.A.G., Steinhof, A., Crummer, K.G., Zimov, N., Zimov, S.A., Heimann, M., Kolle, O., Göckede, M., 2019. Drainage enhances modern soil carbon contribution but reduces old soil carbon contribution to ecosystem respiration in tundra ecosystems. Glob. Chang. Biol. 25 (4), 1315–1325.

Larouche, J.R., Abbott, B.W., Bowden, W.B., Jones, J.B., 2015. The role of watershed characteristics, permafrost thaw, and wildfire on dissolved organic carbon biodegradability and water chemistry in Arctic headwater streams. Biogeosciences 12 (5), 4221–4233.

Laurion, I., Vincent, W.F., Macintyre, S., Retamal, L., Dupont, C., Francus, P., Pienitz, R., 2010. Variability in greenhouse gas emissions from permafrost thaw ponds. Limnol. Oceanogr. 55 (1), 115–133.

Lawrence, D.M., Koven, C.D., Swenson, S.C., Riley, W.J., Slater, A.G., 2015. Permafrost thaw and resulting soil moisture changes regulate projected high-latitude CO_2 and CH_4 emissions. Environ. Res. Lett. 10 (9), 094011.

Li, R., Zhao, L., Ding, Y., Wu, T., Xiao, Y., Du, E., Liu, G., Qiao, Y., 2012. Temporal and spatial variations of the active layer along the Qinghai-Tibet Highway in a permafrost region. Chin. Sci. Bull. 57 (35), 4609–4616.

Li, S., Lü, S., Gao, Y., Ao, Y., 2015. The change of climate and terrestrial carbon cycle over Tibetan Plateau in CMIP5 models. Int. J. Climatol. 35 (14), 4359–4369.

Li, J., Yan, D., Pendall, E., Pei, J., Noh, N.J., He, J.-S., Li, B., Nie, M., Fang, C., 2018a. Depth dependence of soil carbon temperature sensitivity across Tibetan permafrost regions. Soil Biol. Biochem. 126, 82–90.

Li, W., Guo, W., Qiu, B., Xue, Y., Hsu, P.-C., Wei, J., 2018b. Influence of Tibetan Plateau snow cover on East Asian atmospheric circulation at medium-range time scales. Nat. Commun. 9 (1), 4243.

Li, F., Peng, Y., Chen, L., Yang, G., Abbott, B.W., Zhang, D., Fang, K., Wang, G., Wang, J., Yu, J., Liu, L., Zhang, Q., Chen, K., Mohammat, A., Yang, Y., 2020. Warming alters surface soil organic matter composition despite unchanged carbon stocks in a Tibetan permafrost ecosystem. Funct. Ecol. 34 (4), 911–922.

Lin, Z.J., Niu, F.J., Xu, Z.Y., Xu, J., Wang, P., 2011. Thermal regime of a thermokarst lake and its influence on permafrost, Beiluhe Basin, Qinghai-Tibet Plateau. Permafr. Periglac. Process. 21 (4), 315–324.

Ling, F., Zhang, T., 2018. Progress in Numerical Simulation of Long-Term Impact of Thermokarst Lakes on Permafrost Thermal Regime. Adv. Earth Science 33 (2), 115–130.

Ling, F., Wu, Q.B., Niu, F.J., Zhang, T.J., 2012. Modeled response of talik development under thermokarst lakes to permafrost thickness on the Qinghai-Tibet Plateau. Sci. Cold Arid Reg. 6 (6), 521–530.

Liu, W., Chen, S., Qin, X., Baumann, F., Scholten, T., Zhou, Z., Sun, W., Zhang, T., Ren, J., Qin, D., 2012. Storage, patterns, and control of soil organic carbon and nitrogen in the northeastern margin of the Qinghai–Tibetan Plateau. Environ. Res. Lett. 7 (3), 035401.

Liu, F., Chen, L., Abbott, B.W., Xu, Y., Yang, G., Kou, D., Qin, S., Strauss, J., Wang, Y., Zhang, B., Yang, Y., 2018a. Reduced quantity and quality of SOM along a thaw sequence on the Tibetan Plateau. Environ. Res. Lett. 13 (10), 104017.

Liu, F., Chen, L., Zhang, B., Wang, G., Qin, S., Yang, Y., 2018b. Ultraviolet radiation rather than inorganic nitrogen increases dissolved organic carbon biodegradability in a typical thermo-erosion gully on the Tibetan Plateau. Sci. Total Environ. 627, 1276–1284.

Liu, G., Wu, T., Hu, G., Wu, X., Li, W., 2021. Permafrost existence is closely associated with soil organic matter preservation: Evidence from relationships among environmental factors and soil carbon in a permafrost boundary area. Catena 196, 104894.

Loranty, M.M., Abbott, B.W., Blok, D., Douglas, T.A., Epstein, H.E., Forbes, B.C., Jones, B. M., Kholodov, A.L., Kropp, H., Malhotra, A., 2018. Reviews and syntheses: Changing ecosystem influences on soil thermal regimes in northern high-latitude permafrost regions. Biogeosciences 15 (17), 5287–5313.

Lundin, E.J., Giesler, R., Persson, A., Thompson, M.S., Karlsson, J., 2013. Integrating carbon emissions from lakes and streams in a subarctic catchment. J. Geophys. Res. Biogeosci. 118 (3), 1200–1207.

Luo, J., Niu, F., Lin, Z., Liu, M., Yin, G., 2015. Thermokarst lake changes between 1969 and 2010 in the Beilu River Basin, Qinghai–Tibet Plateau, China. Sci. Bull. 60 (5), 556–564.

Luo, J., Niu, F., Lin, Z., Liu, M., Yin, G., 2019. Recent acceleration of thaw slumping in permafrost terrain of Qinghai-Tibet Plateau: An example from the Beiluhe Region. Geomorphology 341, 79–85.

Mack, M.C., Schuur, E.A.G., Bret-Harte, M.S., Shaver, G.R., Chapin, F.S., 2004. Ecosystem carbon storage in arctic tundra reduced by long-term nutrient fertilization. Nature 431 (7007), 440–443.

Mack, M.C., Bret-Harte, M.S., Hollingsworth, T.N., Jandt, R.R., Schuur, E.A.G., Shaver, G. R., Verbyla, D.L., 2011. Carbon loss from an unprecedented Arctic tundra wildfire. Nature 475 (7357), 489–492.

Malone, E.T., Abbott, B.W., Klaar, M.J., Kidd, C., Sebilo, M., Milner, A.M., Pinay, G., 2018. Decline in ecosystem $\delta^{13}C$ and mid-successional nitrogen loss in a Two-Century Postglacial Chronosequence. Ecosystems 1–17.

Mcguire, A.D., Christensen, T.R., Hayes, D., Heroult, A., Euskirchen, E., Kimball, J.S., Koven, C., Lafleur, P., Miller, P.A., Oechel, W., 2012. An assessment of the carbon balance of Arctic tundra: comparisons among observations, process models, and atmospheric inversions. Biogeosciences 9 (8), 3185–3204.

McGuire, A.D., Lawrence, D.M., Koven, C., Clein, J.S., Burke, E., Chen, G., Jafarov, E., MacDougall, A.H., Marchenko, S., Nicolsky, D., Peng, S., Rinke, A., Ciais, P., Gouttevin, I., Hayes, D.J., Ji, D., Krinner, G., Moore, J.C., Romanovsky, V., Schädel, C., Schaefer, K., Schuur, E.A.G., Zhuang, Q., 2018. Dependence of the evolution of carbon dynamics in the northern permafrost region on the trajectory of climate change. Proc. Natl. Acad. Sci. U. S. A. 115 (15), 3882–3887.

Metcalfe, D.B., Hermans, T.D.G., Ahlstrand, J., Becker, M., Berggren, M., Björk, R.G., Björkman, M.P., Blok, D., Chaudhary, N., Chisholm, C., Classen, A.T., Hasselquist, N. J., Jonsson, M., Kristensen, J.A., Kumordzi, B.B., Lee, H., Mayor, J.R., Prevéy, J., Pantazatou, K., Rousk, J., Sponseller, R.A., Sundqvist, M.K., Tang, J., Uddling, J., Wallin, G., Zhang, W., Ahlström, A., Tenenbaum, D.E., Abdi, A.M., 2018. Patchy field sampling biases understanding of climate change impacts across the Arctic. Nat. Ecol. Evol. 2 (9), 1443–1448.

Meyer, N., Welp, G., Amelung, W., 2018. The temperature sensitivity (Q_{10}) of soil respiration: controlling factors and spatial prediction at regional scale based on environmental soil classes. Glob. Biogeochem. Cycles 32 (2), 306–323.

Mikan, C.J., Schimel, J.P., Doyle, A.P., 2002. Temperature controls of microbial respiration in arctic tundra soils above and below freezing. Soil Biol. Biochem. 34 (11), 1785–1795.

Moni, C., Lerch, T.Z., Zarruk, K.K.D., Strand, L.T., Forte, C., Certini, G., Rasse, D.P., 2015. Temperature response of soil organic matter mineralisation in arctic soil profiles. Soil Biol. Biochem. 88, 236–246.

Moon, T.A., Overeem, I., Druckenmiller, M., Holland, M., Huntington, H., Kling, G., Lovecraft, A.L., Miller, G., Scambos, T., Schädel, C., Schuur, E.A.G., Trochim, E., Wiese, F., Williams, D., Wong, G., 2019. The expanding footprint of rapid Arctic change. Earth`s Future 7 (3), 212–218.

Mu, C., Zhang, T., Wu, Q., Peng, X., Cao, B., Zhang, X., Cheng, G., 2015. Organic carbon pools in permafrost regions on the Qinghai–Xizang (Tibetan) Plateau. Cryosphere 9 (2), 479–486.

Mu, C., Zhang, T., Wu, Q., Peng, X., Peng, Z., Yang, Y., Hou, Y., Zhang, X., Cheng, G., 2016a. Dissolved organic carbon, CO2, and CH4 concentrations and their stable isotope ratios in thermokarst lakes on the Qinghai-Tibetan Plateau. J. Limnol. 75 (1-2), 313–319.

Mu, C., Zhang, T., Zhang, X., Cao, B., Peng, X., 2016b. Sensitivity of soil organic matter decomposition to temperature at different depths in permafrost regions on the northern Qinghai-Tibet Plateau. Eur. J. Soil Sci. 67 (6), 773–781.

Mu, C., Zhang, T., Zhang, X., Li, L., Guo, H., Zhao, Q., Cao, L., Wu, Q., Cheng, G., 2016c. Carbon loss and chemical changes from permafrost collapse in the northern Tibetan Plateau. J. Geophys. Res. Biogeosci. 121 (7), 1781–1791.

Mu, C., Zhang, T., Zhao, Q., Su, H., Wang, S., Cao, B., Peng, X., Wu, Q., Wu, X., 2017a. Permafrost affects carbon exchange and its response to experimental warming on the northern Qinghai-Tibetan Plateau. Agric. For. Meteorol. 247, 252–259.

Mu, C.C., Abbott, B.W., Wu, X.D., Zhao, Q., Wang, H.J., Su, H., Wang, S.F., Gao, T.G., Peng, X.Q., Zhang, T.J., 2017b. Thaw depth determines dissolved organic carbon concentration and biodegradability on the northern Qinghai-Tibetan Plateau. Geophys. Res. Lett. 44 (18), 9389–9399.

Mu, C.C., Abbott, B.W., Zhao, Q., Su, H., Wang, S.F., Wu, Q.B., Zhang, T.J., Wu, X.D., 2017c. Permafrost collapse shifts alpine tundra to a carbon source but reduces N_2O and CH_4 release on the northern Qinghai-Tibetan Plateau. Geophys. Res. Lett. 44 (17), 8945–8952.

Mu, C., Li, L., Zhang, F., Li, Y., Xiao, X., Zhao, Q., Zhang, T., 2018. Impacts of permafrost on above- and belowground biomass on the northern Qinghai-Tibetan Plateau. Arct. Antarct. Alp. Res. 50 (1) e1447192.

Mu, C., Schuster, P.F., Abbott, B.W., Kang, S., Guo, J., Sun, S., Wu, Q., Zhang, T., 2020a. Permafrost degradation enhances the risk of mercury release on Qinghai-Tibetan Plateau. Sci. Total Environ. 708, 135127.

Mu, C., Shang, J., Zhang, T., Fan, C., Wang, S., Peng, X., Zhong, W., Zhang, F., Mu, M., Jia, L., 2020b. Acceleration of thaw slump during 1997–2017 in the Qilian Mountains of the northern Qinghai-Tibetan plateau. Landslides 17 (5), 1051–1062.

Mu, C., Zhang, F., Mu, M., Chen, X., Li, Z., Zhang, T., 2020c. Organic carbon stabilized by iron during slump deformation on the Qinghai-Tibetan Plateau. Catena 187, 104282.

Natali, S.M., Watts, J.D., Rogers, B.M., Potter, S., Ludwig, S.M., Selbmann, A.-K., Sullivan, P.F., Abbott, B.W., Arndt, K.A., Birch, L., Björkman, M.P., Bloom, A.A., Celis, G., Christensen, T.R., Christiansen, C.T., Commane, R., Cooper, E.J., Crill, P., Czimczik, C., Davydov, S., Du, J., Egan, J.E., Elberling, B., Euskirchen, E.S., Friborg, T., Genet, H., Göckede, M., Goodrich, J.P., Grogan, P., Helbig, M., Jafarov, E.E., Jastrow, J.D., Kalhori, A.A.M., Kim, Y., Kimball, J.S., Kutzbach, L., Lara, M.J., Larsen, K.S., Lee, B.-Y., Liu, Z., Loranty, M.M., Lund, M., Lupascu, M., Madani, N., Malhotra, A., Matamala, R., McFarland, J., McGuire, A.D., Michelsen, A., Minions, C., Oechel, W.C., Olefeldt, D., Parmentier, F.-J.W., Pirk, N., Poulter, B., Quinton, W., Rezanezhad, F., Risk, D., Sachs, T., Schaefer, K., Schmidt, N.M., Schuur, E.A.G., Semenchuk, P.R., Shaver, G., Sonnentag, O., Starr, G., Treat, C.C., Waldrop, M.P., Wang, Y., Welker, J., Wille, C., Xu, X., Zhang, Z., Zhuang, Q., Zona, D., 2019. Large loss of CO_2 in winter observed across the northern permafrost region. Nat. Clim. Chang. 9 (11), 852–857.

Nitze, I., Grosse, G., Jones, B.M., Arp, C.D., Ulrich, M., Federov, A., Veremeeva, A., 2017. Landsat-based trend analysis of lake dynamics across northern permafrost regions. Remote Sens. 9 (7), 640.

Niu, F., Cheng, G., Ni, W., Jin, D., 2005. Engineering-related slope failure in permafrost regions of the Qinghai-Tibet Plateau. Cold Reg. Sci. Technol. 42 (3), 215–225.

Niu, F., Luo, J., Lin, Z., Ma, W., Lu, J., 2012. Development and thermal regime of a thaw slump in the Qinghai–Tibet plateau. Cold Reg. Sci. Technol. 83, 131–138.

Niu, F., Luo, J., Lin, Z., Liu, M., Yin, G., 2014. Thaw-induced slope failures and susceptibility mapping in permafrost regions of the Qinghai–Tibet Engineering Corridor, China. Nat. Hazards 74 (3), 1667–1682.

Obu, J., Westermann, S., Bartsch, A., Berdnikov, N., Christiansen, H.H., Dashtseren, A., Delaloye, R., Elberling, B., Etzelmüller, B., Kholodov, A., Khomutov, A., Kääb, A., Leibman, M.O., Lewkowicz, A.G., Panda, S.K., Romanovsky, V., Way, R.G., Westergaard-Nielsen, A., Wu, T., Yamkhin, J., Zou, D., 2019. Northern Hemisphere permafrost map based on TTOP modelling for 2000–2016 at 1 km^2 scale. Earth Sci. Rev. 193, 299–316.

Olefeldt, D., Devito, K.J., Turetsky, M.R., 2013. Sources and fate of terrestrial dissolved organic carbon in lakes of a Boreal Plains region recently affected by wildfire. Biogeosciences 10, 6247–6265.

Olefeldt, D., Goswami, S., Grosse, G., Hayes, D., Hugelius, G., Kuhry, P., McGuire, A.D., Romanovsky, V.E., Sannel, A.B., Schuur, E.A., Turetsky, M.R., 2016. Circumpolar distribution and carbon storage of thermokarst landscapes. Nat. Commun. 7, 13043.

Pang, Q., Zhao, L., Li, S., Ding, Y., 2012. Active layer thickness variations on the Qinghai–Tibet Plateau under the scenarios of climate change. Environ. Earth Sci. 66 (3), 849–857.

Pearce, A.R., Rastetter, E.B., Kwiatkowski, B.L., Bowden, W.B., Mack, M.C., Jiang, Y., 2015. Recovery of arctic tundra from thermal erosion disturbance is constrained by nutrient accumulation: a modeling analysis. Ecol. Appl. 25 (5), 1271–1289.

Peng, X., Zhang, T., Frauenfeld, O.W., Wang, K., Luo, D., Cao, B., Su, H., Jin, H., Wu, Q., 2018. Spatiotemporal changes in active layer thickness under contemporary and projected climate in the Northern Hemisphere. J. Clim. 31 (1), 251–266.

Pepin, N., Bradley, R., Diaz, H., Baraer, M., Caceres, E., Forsythe, N., Fowler, H., Greenwood, G., Hashmi, M., Liu, X., 2015. Elevation-dependent warming in mountain regions of the world. Nat. Clim. Chang. 5 (5), 424–430.

Piao, S., Fang, J., Ciais, P., Peylin, P., Huang, Y., Sitch, S., Wang, T., 2009. The carbon balance of terrestrial ecosystems in China. Nature 458 (7241), 1009–1013.

Piao, S., Tan, K., Nan, H., Ciais, P., Fang, J., Wang, T., Vuichard, N., Zhu, B., 2012. Impacts of climate and CO2 changes on the vegetation growth and carbon balance of Qinghai–Tibetan grasslands over the past five decades. Glob. Planet. Chang. 98, 73–80.

Piao, S., Wang, X., Park, T., Chen, C., Lian, X., He, Y., Bjerke, J.W., Chen, A., Ciais, P., Tømmervik, H., Nemani, R.R., Myneni, R.B., 2020. Characteristics, drivers and feedbacks of global greening. Nat. Rev. Earth Environ. 1, 14–27.

Ping, C., Michaelson, G.J., Jorgenson, M.T., Kimble, J.M., Epstein, H., Romanovsky, V.E., Walker, D.A., 2008a. High stocks of soil organic carbon in the North American Arctic region. Nat. Geosci. 1 (9), 615–619.

Ping, C.L., Michaelson, G.J., Kimble, J.M., Romanovsky, V.E., Shur, Y.L., Swanson, D.K., Walker, D.A., 2008b. Cryogenesis and soil formation along a bioclimate gradient in Arctic North America. J. Geophys. Res. Biogeosci. 113 (G3). G03S12.

Polvani, L.M., Previdi, M., England, M.R., Chiodo, G., Smith, K.L., 2020. Substantial twentieth-century Arctic warming caused by ozone-depleting substances. Nat. Clim. Chang. 10 (2), 130–133.

Qin, Y., Yi, S., Chen, J., Ren, S., Wang, X., 2015. Responses of ecosystem respiration to short-term experimental warming in the alpine meadow ecosystem of a permafrost site on the Qinghai–Tibetan Plateau. Cold Reg. Sci. Technol. 115, 77–84.

Qin, Y., Wu, T., Zhao, L., Wu, X., Li, R., Xie, C., Pang, Q., Hu, G., Qiao, Y., Zhao, G., Liu, G., Zhu, X., Hao, J., 2017. Numerical modeling of the active layer thickness and permafrost thermal state across Qinghai-Tibetan Plateau. J. Geophys. Res.-Atmos. 122 (21), 11604–11620.

Qin, S., Chen, L., Fang, K., Zhang, Q., Wang, J., Liu, F., Yu, J., Yang, Y., 2019. Temperature sensitivity of SOM decomposition governed by aggregate protection and microbial communities. Sci. Adv. 5 (7) eaau1218.

Qu, B., Sillanpää, M., Li, C., Kang, S., Stubbins, A., Yan, F., Aho, K.S., Zhou, F., Raymond, P.A., 2017. Aged dissolved organic carbon exported from rivers of the Tibetan Plateau. PLoS One 12 (5), e0178166.

Quan, Q., Tian, D., Luo, Y., Zhang, F., Crowther, T.W., Zhu, K., Chen, H.Y.H., Zhou, Q., Niu, S., 2019. Water scaling of ecosystem carbon cycle feedback to climate warming. Sci. Adv. 5 (8) eaav1131.

Rasmussen, C., Heckman, K., Wieder, W.R., Keiluweit, M., Lawrence, C.R., Berhe, A.A., Blankinship, J.C., Crow, S.E., Druhan, J.L., Hicks Pries, C.E., Marin-Spiotta, E., Plante, A.F., Schädel, C., Schimel, J.P., Sierra, C.A., Thompson, A., Wagai, R., 2018. Beyond clay: towards an improved set of variables for predicting soil organic matter content. Biogeochemistry 137 (3), 297–306.

Raymond, P.A., Hartmann, J., Lauerwald, R., Sobek, S., Mcdonald, C.P., Hoover, M.D., Butman, D., Striegl, R., Mayorga, E., Humborg, C., 2013. Global carbon dioxide emissions from inland waters. Nature 503 (7476), 355–359.

Schädel, C., Bader, M.K.F., Schuur, E.A.G., Biasi, C., Bracho, R., Capek, P., De Baets, S., Diakova, K., Ernakovich, J., Estoparagones, C., 2016. Potential carbon emissions dominated by carbon dioxide from thawed permafrost soils. Nat. Clim. Chang. 6 (10), 950–953.

Schädel, C., Schuur, E.A.G., Bracho, R., Elberling, B., Knoblauch, C., Lee, H., Luo, Y., Shaver, G.R., Turetsky, M.R., 2014. Circumpolar assessment of permafrost C quality and its vulnerability over time using long-term incubation data. Glob. Chang. Biol. 20 (2), 641–652.

Schmitz, O.J., Raymond, P.A., Estes, J.A., Kurz, W.A., Holtgrieve, G.W., Ritchie, M.E., Schindler, D.E., Spivak, A.C., Wilson, R.W., Bradford, M.A., Christensen, V., Deegan, L., Smetacek, V., Vanni, M.J., Wilmers, C.C., 2014. Animating the Carbon Cycle. Ecosystems 17 (2), 344–359.

Schuur, E., McGuire, A., Schädel, C., Grosse, G., Harden, J., Hayes, D., Hugelius, G., Koven, C., Kuhry, P., Lawrence, D., 2015. Climate change and the permafrost carbon feedback. Nature 520 (7546), 171–179.

Shang, W., Wu, X., Zhao, L., Yue, G., Zhao, Y., Qiao, Y., Li, Y., 2016. Seasonal variations in labile soil organic matter fractions in permafrost soils with different vegetation types in the central Qinghai–Tibet Plateau. Catena 137, 670–678.

Shaver, G.R., Bret-Harte, M.S., Jones, M.H., Johnstone, J., Gough, L., Laundre, J., Chapin III, F.S., 2001. Species composition interacts with fertilizer to control long-term change in tundra productivity. Ecology 82 (11), 3163–3181.

Shogren, A.J., Zarnetske, J.P., Abbott, B.W., Iannucci, F., Frei, R.J., Griffin, N.A., Bowden, W.B., 2019. Revealing biogeochemical signatures of Arctic landscapes with river chemistry. Sci. Rep. 9 (1), 12894.

Shogren, A.J., Zarnetske, J.P., Abbott, B.W., Iannucci, F., Bowden, W.B., 2020. We cannot shrug off the shoulder seasons: Addressing knowledge and data gaps in an Arctic Headwater. Environ. Res. Lett. 15 (10), 104027.

Shur, Y.L., Jorgenson, M.T., 2007. Patterns of permafrost formation and degradation in relation to climate and ecosystems. Permafr. Periglac. Process. 18 (1), 7–19.

Song, W., Wang, H., Wang, G., Chen, L., Jin, Z., Zhuang, Q., He, J.S., 2015. Methane emissions from an alpine wetland on the Tibetan Plateau: Neglected but vital contribution of the nongrowing season. J. Geophys. Res. Biogeosci. 120 (8), 1475–1490.

Spencer, R.G.M., Guo, W., Raymond, P.A., Dittmar, T., Hood, E., Fellman, J., Stubbins, A., 2014. Source and biolability of ancient dissolved organic matter in glacier and lake ecosystems on the Tibetan Plateau. Geochim. Cosmochim. Acta 142, 64–74.

Strauss, J., Schirrmeister, L., Grosse, G., Fortier, D., Hugelius, G., Knoblauch, C., Romanovsky, V., Schädel, C., Deimling, T.S.V., Schuur, E.A.G., 2017. Deep Yedoma permafrost: A synthesis of depositional characteristics and carbon vulnerability. Earth Sci. Rev. 172, 75–86.

Sun, Z., Wang, Y., Sun, Y., Niu, F., Li, Guoyu, Gao, Z., 2017. Creep characteristics and process analyses of a thaw slump in the permafrost region of the Qinghai-Tibet Plateau, China. Geomorphology 293, 1–10.

Tank, S.E., Vonk, J.E., Walvoord, M.A., McClelland, J.W., Laurion, I., Abbott, B.W., 2020. Landscape matters: Predicting the biogeochemical effects of permafrost thaw on aquatic networks with a state factor approach. Permafr. Periglac. Process. 31 (3), 358–370.

Tanski, G., Lantuit, H., Ruttor, S., Knoblauch, C., Radosavljevic, B., Strauss, J., Wolter, J., Irrgang, A.M., Ramage, J., Fritz, M., 2017. Transformation of terrestrial organic matter along thermokarst-affected permafrost coasts in the Arctic. Sci. Total Environ. 581–582, 434–447.

Tarnocai, C., Canadell, J.G., Schuur, E.A.G., Kuhry, P., Mazhitova, G., Zimov, S., 2009. Soil organic carbon pools in the northern circumpolar permafrost region. Glob. Biogeochem. Cycles 23 (2). GB2023.

Tian, L., Zhao, L., Wu, X., Fang, H., Zhao, Y., Yue, G., Liu, G., Chen, H., 2017. Vertical patterns and controls of soil nutrients in alpine grassland: Implications for nutrient uptake. Sci. Total Environ. 607-608, 855–864.

Tian, L., Zhao, L., Wu, X., Hu, G., Fang, H., Zhao, Y., Sheng, Y., Chen, J., Wu, J., Li, W., Ping, C.-L., Pang, Q., Liu, Y., Shi, W., Wu, T., Zhang, X., 2019. Variations in soil nutrient availability across Tibetan grassland from the 1980s to 2010s. Geoderma 338, 197–205.

Torn, M.S., Trumbore, S.E., Chadwick, O.A., Vitousek, P.M., Hendricks, D.M., 1997. Mineral control of soil organic carbon storage and turnover. Nature 389 (6647), 170–173.

Treat, C.C., Wollheim, W.M., Varner, R.K., Grandy, A.S., Talbot, J., Frolking, S., 2014. Temperature and peat type control CO_2 and CH_4 production in Alaskan permafrost peats. Glob. Chang. Biol. 20 (8), 2674–2686.

Treat, C.C., Natali, S.M., Ernakovich, J., Iversen, C.M., Lupascu, M., Mcguire, A.D., Norby, R.J., Chowdhury, T.R., Richter, A., Santrůčkova, H., 2015. A pan-Arctic synthesis of CH4 and CO2 production from anoxic soil incubations. Glob. Chang. Biol. 21 (7), 2787–2803.

Trumbore, S.E., 1997. Potential responses of soil organic carbon to global environmental change. Proc. Natl. Acad. Sci. U. S. A. 94 (16), 8284–8291.

Turetsky, M.R., Abbott, B.W., Jones, M.C., Anthony, K.W., Olefeldt, D., Schuur, E.A.G., Grosse, G., Kuhry, P., Hugelius, G., Koven, C., Lawrence, D.M., Gibson, C., Sannel, A. B.K., McGuire, A.D., 2020. Carbon release through abrupt permafrost thaw. Nat. Geosci. 13 (2), 138–143.

Väisänen, M., Ylänne, H., Kaarlejärvi, E., Sjögersten, S., Olofsson, J., Crout, N., Stark, S., 2014. Consequences of warming on tundra carbon balance determined by reindeer grazing history. Nat. Clim. Chang. 4, 384–388.

Vaks, A., Mason, A.J., Breitenbach, S.F.M., Kononov, A.M., Osinzev, A.V., Rosensaft, M., Borshevsky, A., Gutareva, O.S., Henderson, G.M., 2020. Palaeoclimate evidence of vulnerable permafrost during times of low sea ice. Nature 577 (7789), 221–225.

Voigt, C., Marushchak, M.E., Abbott, B.W., Biasi, C., Elberling, B., Siciliano, S.D., Sonnentag, O., Stewart, K.J., Yang, Y., Martikainen, P.J., 2020. Nitrous oxide emissions from permafrost-affected soils. Nat. Rev. Earth Environ. 1 (8), 420–434.

Vonk, J.E., Tank, S.E., Mann, P.J., Spencer, R.G.M., Treat, C.C., Striegl, R.G., Abbott, B. W., Wickland, K.P., 2015. Biodegradability of dissolved organic carbon in permafrost soils and aquatic systems: a meta-analysis. Biogeosciences 12 (23), 6915–6930.

Vonk, J.E., Tank, S.E., Walvoord, M.A., 2019. Integrating hydrology and biogeochemistry across frozen landscapes. Nat. Commun. 10 (1), 5377.

Waldrop, M.P., Wickland, K.P., Iii, R.W., Berhe, A.A., Harden, J.W., Romanovsky, V.E., 2010. Molecular investigations into a globally important carbon pool: permafrost-protected carbon in Alaskan soils. Glob. Chang. Biol. 16 (9), 2543–2554.

Walter Anthony, K., Daanen, R., Anthony, P., Schneider von Deimling, T., Ping, C.-L., Chanton, J.P., Grosse, G., 2016. Methane emissions proportional to permafrost carbon thawed in Arctic lakes since the 1950s. Nat. Geosci. 9, 679–682.

Wang, G., Qian, J., Cheng, G., Lai, Y., 2002. Soil organic carbon pool of grassland soils on the Qinghai-Tibetan Plateau and its global implication. Sci. Total Environ. 291 (1-3), 207–217.

Wang, X., Yang, M., Liang, X., Pang, G., Wan, G., Chen, X., Luo, X., 2014. The dramatic climate warming in the Qaidam Basin, northeastern Tibetan Plateau, during 1961–2010. Int. J. Climatol. 34 (5), 1524–1537.

Wang, Z., Wang, Q., Zhao, L., Wu, X., Yue, G., Zou, D., Nan, Z., Liu, G., Pang, Q., Fang, H., Wu, T., Shi, J., Jiao, K., Zhao, Y., Zhang, L., 2016. Mapping the vegetation distribution of the permafrost zone on the Qinghai-Tibet Plateau. J. Mt. Sci. 13 (6), 1035–1046.

Wang, K., Zhang, T., Zhang, X., Clow, G.D., Jafarov, E.E., Overeem, I., Romanovsky, V., Peng, X., Cao, B., 2017. Continuously amplified warming in the Alaskan Arctic: Implications for estimating global warming hiatus. Geophys. Res. Lett. 44 (17), 9029–9038.

Wang, X., Pang, G., Yang, M., 2018a. Precipitation over the Tibetan Plateau during recent decades: a review based on observations and simulations. Int. J. Climatol. 38 (3), 1116–1131.

Wang, Y., Sun, Z., Sun, Y., 2018b. Effects of a thaw slump on active layer in permafrost regions with the comparison of effects of thermokarst lakes on the Qinghai-Tibet Plateau, China. Geoderma 314 (14), 47–57.

Wang, N., Quesada, B., Xia, L., Butterbach-Bahl, K., Goodale, C.L., Kiese, R., 2019. Effects of climate warming on carbon fluxes in grasslands—A global meta-analysis. Glob. Chang. Biol. 25 (5), 1839–1851.

Wang, T., Yang, D., Yang, Y., Piao, S., Li, X., Cheng, G., Fu, B., 2020. Permafrost thawing puts the frozen carbon at risk over the Tibetan Plateau. Sci. Adv. 6 (19) eaaz3513.

Weege, S., Lantuit, H., Fritz, M., Obu, J., Radosavljevic, B., 2014. Impact of climatic forces on the thawing process of a retrogressive thaw slump and its sediment and carbon release on the Yukon Coast, Canada. In: 4th European Conference on Permafrost. Évora, Portugal.

Whalen, S., 2005. Biogeochemistry of methane exchange between natural wetlands and the atmosphere. Environ. Eng. Sci. 22 (1), 73–94.

Wickland, K.P., Neff, J.C., 2008. Decomposition of soil organic matter from boreal black spruce forest: environmental and chemical controls. Biogeochemistry 87 (1), 29–47.

Wild, B., Schnecker, J., Alves, R.J.E., Barsukov, P., Bárta, J., Čapek, P., Gentsch, N., Gittel, A., Guggenberger, G., Lashchinskiy, N., Mikutta, R., Rusalimova, O., Šantrůčková, H., Shibistova, O., Urich, T., Watzka, M., Zrazhevskaya, G., Richter, A., 2014. Input of easily available organic C and N stimulates microbial decomposition of soil organic matter in arctic permafrost soil. Soil Biol. Biochem. 75, 143–151.

Wu, Q., Zhang, T., 2008. Recent permafrost warming on the Qinghai–Tibet Plateau. J. Geophys. Res.-Atmos. 113, D13108.

Wu, Q., Zhang, T., 2010. Changes in active layer thickness over the Qinghai-Tibetan Plateau from 1995 to 2007. J. Geophys. Res.-Atmos. 115 (D9), D9107.

Wu, Q., Zhang, T., Liu, Y., 2010. Permafrost temperatures and thickness on the Qinghai-Tibet Plateau. Glob. Planet. Chang. 72 (1), 32–38.

Wu, Q., Zhang, T., Liu, Y., 2012. Thermal state of the active layer and permafrost along the Qinghai-Xizang (Tibet) Railway from 2006 to 2010. Cryosphere 6 (3), 607–612.

Wu, Q., Zhang, P., Jiang, G., Yang, Y., Deng, Y., Wang, X., 2014a. Bubble emissions from thermokarst lakes in the Qinghai–Xizang Plateau. Quat. Int. 321, 65–70.

Wu, X., Fang, H., Zhao, L., Wu, T., Li, R., Ren, Z., Pang, Q., Ding, Y., 2014b. Mineralisation and changes in the fractions of soil organic matter in soils of the permafrost region, Qinghai-Tibet Plateau, China. Permafr. Periglac. Process. 25 (1), 35–44.

Wu, Q., Hou, Y., Yun, H., Liu, Y., 2015. Changes in active-layer thickness and near-surface permafrost between 2002 and 2012 in alpine ecosystems, Qinghai–Xizang (Tibet) Plateau, China. Glob. Planet. Chang. 124, 149–155.

Wu, X., Zhao, L., Fang, H., Zhao, Y., Smoak, J.M., Pang, Q., Ding, Y., 2016. Environmental controls on soil organic carbon and nitrogen stocks in the high-altitude arid western Qinghai-Tibetan Plateau permafrost region. J. Geophys. Res. Biogeosci. 121 (1), 176–187.

Wu, X., Fang, H., Zhao, Y., Smoak, J.M., Li, W., Shi, W., Sheng, Y., Zhao, L., Ding, Y., 2017a. A conceptual model of the controlling factors of soil organic carbon and nitrogen densities in a permafrost-affected region on the eastern Qinghai-Tibetan Plateau. J. Geophys. Res. Biogeosci. 122 (7), 1705–1717.

Wu, X., Xu, H., Liu, G., Zhao, L., Mu, C., 2018a. Effects of permafrost collapse on soil bacterial communities in a wet meadow on the northern Qinghai-Tibetan Plateau. BioMed Central Ecol. 18 (1), 27.

Wu, X.D., Zhao, L., Hu, G.J., Liu, G.M., Li, W.P., Ding, Y.J., 2018. Permafrost and land cover as controlling factors for light fraction organic matter on the southern Qinghai-Tibetan Plateau. Sci. Total Environ. 613-614, 1165–1174.

Wu, X., Zhao, L., Liu, G., Xu, H., Zhang, X., Ding, Y., 2018b. Effects of permafrost thaw-subsidence on soil bacterial communities in the southern Qinghai-Tibetan Plateau. Appl. Soil Ecol. 128, 81–88.

Xu, M., Xue, X., 2013. A research on summer vegetation characteristics & short-time responses to experimental warming of alpine meadow in the Qinghai-Tibetan Plateau. Acta Ecol. Sin. 33 (7), 2071–2083.

Xu, H.Y., Liu, G.M., Wu, X.D., Smoak, J.M., Mu, C.C., Ma, X.L., Zhang, X.L., Li, H.Q., Hu, G.L., 2018. Soil enzyme response to permafrost collapse in the Northern Qinghai-Tibetan Plateau. Ecol. Indic. 85, 585–593.

Yan, L., Zhou, G.S., Wang, Y.H., Hu, T.Y., Sui, X.H., 2015. The spatial and temporal dynamics of carbon budget in the alpine grasslands on the Qinghai-Tibetan Plateau using the Terrestrial Ecosystem Model. J. Clean. Prod. 107, 195–201.

Yan, F., Sillanpaa, M., Kang, S., Aho, K.S., Qu, B., Wei, D., Li, X., Li, C., Raymond, P.A., 2018. Lakes on the Tibetan Plateau as Conduits of Greenhouse Gases to the Atmosphere. J. Geophys. Res. Biogeosci. 123 (7), 2091–2103.

Yang, Y., Mohammat, A., Feng, J., Zhou, R., Fang, J., 2007. Storage, patterns and environmental controls of soil organic carbon in China. Biogeochemistry 84 (2), 131–141.

Yang, Y., Fang, J., Tang, Y., Ji, C., Zheng, C., He, J., Zhu, B., 2008. Storage, patterns and controls of soil organic carbon in the Tibetan grasslands. Glob. Chang. Biol. 14 (7), 1592–1599.

Yang, Y., Fang, J., Ji, C., Ma, W., Su, S., Tang, Z., 2010. Soil inorganic carbon stock in the Tibetan alpine grasslands. Glob. Biogeochem. Cycles 24 (4). GB4022.

Yang, G., Peng, Y., Olefeldt, D., Chen, Y., Wang, G., Li, F., Zhang, D., Wang, J., Yu, J., Liu, L., 2017. Changes in methane flux along a permafrost thaw sequence on the Tibetan Plateau. Environ. Sci. Technol. 52 (3), 1244–1252.

Yang, Y., Hopping, K.A., Wang, G., Chen, J., Klein, J.A., 2018. Permafrost and drought regulate vulnerability of Tibetan Plateau grasslands to warming. Ecosphere 9 (5), e02233.

Yang, M., Wang, X., Pang, G., Wan, G., Liu, Z., 2019. The Tibetan Plateau cryosphere: Observations and model simulations for current status and recent changes. Earth Sci. Rev. 190, 353–369.

Yi, S., Xiang, B., Meng, B., Wu, X., Ding, Y., 2019. Modeling the carbon dynamics of alpine grassland in the Qinghai-Tibetan Plateau under scenarios of 1.5 and 2°C global warming. Adv. Clim. Chang. Res. 10 (2), 80–91.

Yu, H., Luedeling, E., Chapin, J.X.S., 2010. Winter and spring warming result in delayed spring phenology on the Tibetan Plateau. Proc. Natl. Acad. Sci. U. S. A. 107 (51), 22151–22156.

Yu, L., Wang, H., Wang, Y., Zhang, Z., Chen, L., Liang, N., He, J.-S., 2020. Temporal variation in soil respiration and its sensitivity to temperature along a hydrological gradient in an alpine wetland of the Tibetan Plateau. Agric. For. Meteorol. 282, 107854.

Yuan, Z.-Q., Epstein, H., Li, G.-Y., 2020. Grazing exclusion did not affect soil properties in alpine meadows in the Tibetan permafrost region. Ecol. Eng. 147, 105657.

Yun, H., Wu, Q., Zhuang, Q., Chen, A., Yu, T., Lyu, Z., Yang, Y., Jin, H., Liu, G., Qu, Y., Liu, L., 2018. Consumption of atmospheric methane by the Qinghai–Tibet Plateau alpine steppe ecosystem. Cryosphere 12 (9), 2803–2819.

Zarnetske, J.P., Bouda, M., Abbott, B.W., Saiers, J., Raymond, P.A., 2018. Generality of hydrologic transport limitation of watershed organic carbon flux across ecoregions of the United States. Geophys. Res. Lett. 45 (21), 11702–22711.

Zhang, T., Zhong, X., 2014. Classification and regionalization of the seasonal snow cover across the Eurasian Continent. J. Glaciol. Geocryol. 36 (3), 481–490.

Zhang, G., Zhang, Y., Dong, J., Xiao, X., 2013. Green-up dates in the Tibetan Plateau have continuously advanced from 1982 to 2011. Proc. Natl. Acad. Sci. U. S. A. 110 (11), 4309–4314.

Zhang, G., Li, J., Zheng, G., 2017a. Lake-area mapping in the Tibetan Plateau: an evaluation of data and methods. Int. J. Remote Sens. 38 (3-4), 742–772.

Zhang, T., Wang, G., Yan, Y., Mao, T., Chen, X., 2017b. Grassland types and season-dependent response of ecosystem respiration to experimental warming in a permafrost region in the Tibetan Plateau. Agric. For. Meteorol. 247, 271–279.

Zhang, G., Nan, Z., Wu, X., Ji, H., Zhao, S., 2019a. The Role of Winter Warming in Permafrost Change Over the Qinghai-Tibet Plateau. Geophys. Res. Lett. 46 (20), 11261–11269.

Zhang, Q., Yang, G., Song, Y., Kou, D., Wang, G., Zhang, D., Qin, S., Mao, C., Feng, X., Yang, Y., 2019c. Magnitude and drivers of potential methane oxidation and production across the Tibetan alpine permafrost region. Environ. Sci. Technol. 53 (24), 14243–14252.

Zhao, Z., Dong, S., Jiang, X., Liu, S., Ji, H., Li, Y., Han, Y., Sha, W., 2017. Effects of warming and nitrogen deposition on CH4, CO2 and N2O emissions in alpine grassland ecosystems of the Qinghai-Tibetan Plateau. Sci. Total Environ. 592, 565–572.

Zhao, L., Wu, X., Wang, Z., Sheng, Y., Fang, H., Zhao, Y., Hu, G., Li, W., Pang, Q., Shi, J., Mo, B., Wang, Q., Ruan, X., Li, X., Ding, Y., 2018. Soil organic carbon and total nitrogen pools in permafrost zones of the Qinghai-Tibetan Plateau. Sci. Rep. 8 (1), 3656.

Zhao, L., Hu, G., Zou, D., Wu, X., Ma, L., Sun, Z., Yuan, L., Zhou, H., Liu, S., 2019. Permafrost Changes and Its Effects on Hydrological Processes on Qinghai-Tibet Plateau. Bull. Chin. Acad. Sci. 34 (11), 1233–1246.

Zhuang, Q., Melillo, J.M., Kicklighter, D.W., Prinn, R.G., McGuire, A.D., Steudler, P.A., Felzer, B.S., Hu, S., 2004. Methane fluxes between terrestrial ecosystems and the atmosphere at northern high latitudes during the past century: A retrospective analysis with a process-based biogeochemistry model. Glob. Biogeochem. Cycles 18. GB3010.

Zhuang, Q., He, J., Lu, Y., Ji, L., Xiao, J., Luo, T., 2010. Carbon dynamics of terrestrial ecosystems on the Tibetan Plateau during the 20th century: an analysis with a process-based biogeochemical model. Glob. Ecol. Biogeogr. 19 (5), 649–662.

Zong, N., Chai, X., Shi, P., Yang, X., 2017. Effects of warming and nitrogen addition on plant photosynthate partitioning in an Alpine Meadow on the Tibetan Plateau. J. Plant Growth Regul. 37 (3), 803–812.

Zou, D., Zhao, L., Sheng, Y., Chen, J., Hu, G., Wu, T., Wu, J., Xie, C., Wu, X., Pang, Q., Wang, W., Du, E., Li, W., Liu, G., Li, J., Qin, Y., Qiao, Y., Wang, Z., Shi, J., Cheng, G., 2017. A new map of permafrost distribution on the Tibetan Plateau. Cryosphere 11 (6), 2527–2542.